Ceramic Technology at Wadi Fidan 61, an Early Pottery Neolithic Site (ca. 6500 B.C.E.) in the Faynan Region of Southern Jordan

Margie M. Burton[1], Patrick S. Quinn[2], Kathleen Bennallack[1], Alan Farahani[3], Matthew D. Howland[1], Mohammad Najjar[1] and Thomas E. Levy[1]

Abstract

The Faynan region of southern Jordan became a center of industrial-scale metallurgical production during the Bronze and Iron Ages. However, socio-economic developments of the Pottery Neolithic period (ca. 6500-5500 B. C. E.) in the Faynan that helped set the stage for the rise of complex copper-producing societies are not well-understood. In this paper, we focus on ceramic technology at the early Pottery Neolithic site of Wadi Fidan 61 in the western part of the Faynan region. The composition of 38 diagnostic pottery sherds is characterized using an analytical approach that integrates petrography, instrumental geochemistry and Scanning Electron Microscopy-Energy Dispersive X-Ray Spectroscopy along with macroscopic examination. Results indicate six distinct clay recipes and suggest the use of different clay deposits and tempering materials from locations within ca. 5 km of the site. Implications of this compositionally diverse pottery assemblage are considered, possibly linking this initial phase of ceramic production in the Faynan with a kind of foraging-farming economy.

Keywords: Pottery Neolithic; southern Jordan; Faynan; Wadi Fidan; ceramic composition; ceramic technology; provenance

---

[1]Department of Anthropology, University of California San Diego; [2]Institute of Archaeology, University College London; [3]Department of Anthropology, University of Nevada Las Vegas

Margie M. Burton (corresponding author) Department of Anthropology, University of California San Diego, 9500 Gilman Drive, La Jolla, California 92093, USA. Email: mburton@ucsd.edu

1. Introduction

The Faynan region of southern Jordan, located ca. 50 km southeast of the Dead Sea, is arguably best known for its role in the rise of the copper trade and industrial-scale metallurgical production since the Chalcolithic period (ca. 4500-3500 B.C.E.) (e.g. Hauptmann and Weisgerber 1987; Levy 2007; Levy et al. 2014). However, importantly for understanding technological and social developments over the *longue durée,* the Faynan has been inhabited since the Paleolithic and is a recognized zone of Neolithic period occupation (ca. 8500-4500 B.C.E.) that evidences the transition to settled farming economies (Banning 2019; Gopher 2012; Kuijt and Chesson 2002; Levy et al. 2001; Rollefson 2008). Wadi Faynan 16 in the eastern part of the Faynan region, is one of the most important Pre-Pottery Neolithic A (PPNA) sites in the southern Levant (Barker et al. 2007; Finlayson and Mithen 2007; Finlayson et al. 2011). Surveys carried out in that area in the late 1980s revealed a large Middle PPNB site at Ghwair I on a secondary drainage that empties into the Wadi Faynan (Simmons and Najjar 2006). Tell Wadi Feinan was excavated and identified as a Late Neolithic/early Chalcolithic site (Najjar et al. 1990). The Southern Ghors and Northeast Arabah Survey (Macdonald 1987, 1992; MacDonald et al. 1988) reached the western part of the Faynan region including sites in the Arabah Valley previously recorded by Raikes (1980, 1985) in the Wadi Fidan gorge. Four Neolithic sites were identified in Wadi Fidan; three had associated architecture and abundant lithics indicating intensive habitation (MacDonald 1992). According to MacDonald (1992: 37), the Wadi Fidan was one of few "core areas" of Neolithic settlement within the survey area and, based on projectile point morphology, the Wadi Fidan Neolithic sites might represent occupation on "either side" of the Pre-Pottery Neolithic (PPN)--Pottery Neolithic (PN) transition. Wadi Feifa, ca. 30 km to the north, appeared to be a second "core area" of Pottery Neolithic settlement. Springs and/or perennial streams were present in both areas and were likely important factors influencing location and continuity of settlement.

The Wadi Fidan drainage was most recently systematically surveyed by Levy et al. (2001) as part of the University of California San Diego – Department of Antiquities of Jordan Edom Lowlands Regional Archaeology Project (ELRAP). This survey recorded a total of 125 sites dating from the Paleolithic to the Islamic period along the westernmost 4.5 km course of the drainage (Levy et al. 2001: 174, Fig. 10, 175, Table 2). Wadi Fidan 61, on the south bank, was one of four Neolithic habitation sites identified and was excavated in 2012. Wadi Fidan 61 had been previously recorded by Raikes (1980) as "Site C" and by MacDonald (1992) as two sites, "Site 44" and "Site 15", on the eastern and western slopes respectively of granitic outcrops. Other nearby excavated Neolithic sites include Late PPNB/PPNC Wadi Fidan 01 (Tel Tif'dan, Twiss 2007) and PN Wadi Fidan 51 (Levy et al. 2001) (Fig. 1).

As one of few excavated Pottery Neolithic sites in the Faynan region, Wadi Fidan 61 holds potential to advance our understanding of early pottery production in this part of the southern Levant. In particular, detailed studies of ceramic composition from sites of this time frame in the Faynan region are almost totally lacking. Goren (1990) has reported petrographic analyses of some surface finds "with no clear archaeological context". Iron Age pottery from Faynan sites has been more intensively studied including petrographic and geochemical studies (Gunneweg and Balla 2002; Smith et al. 2014). The aim of this paper is to investigate ceramic technology at Pottery Neolithic Wadi Fidan 61 using an analytical approach integrating petrography, instrumental geochemistry, and Scanning Electron Microscopy-Energy Dispersive

X-Ray Spectroscopy (SEM-EDS) with macroscopic examination. By relating ceramic composition to the local geology, we assess where and how raw materials were procured and prepared to manufacture pottery vessels. We then consider the implications of the results for understanding socio-economic organization at Wadi Fidan 61. The detailed data provide a baseline for future comparative studies that may help to illuminate connections between sites and local diachronic development of ceramic technology.

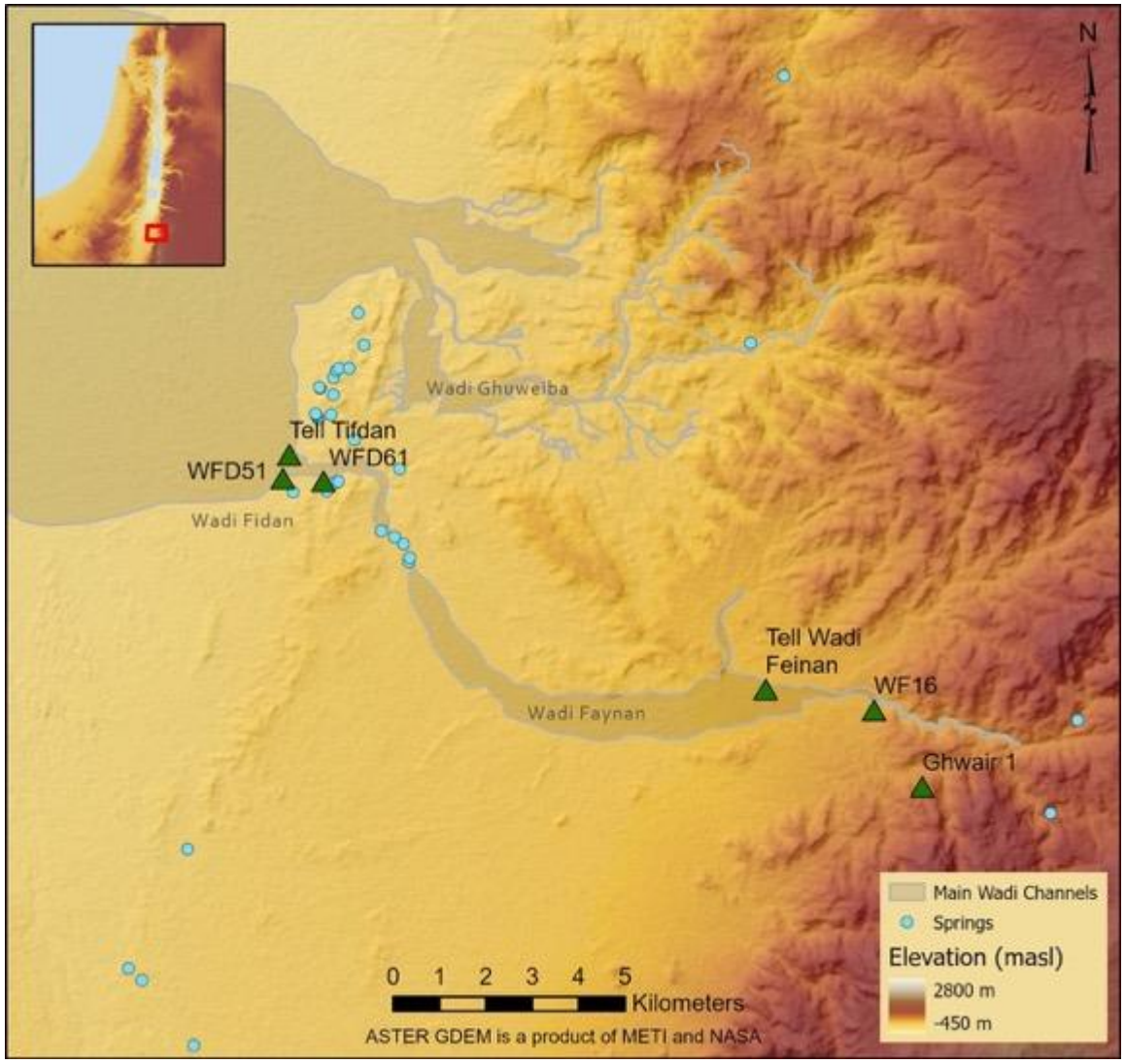

Figure 1. Elevation map showing excavated Neolithic sites within the Faynan study area in southern Jordan (Levy et al. 2001). PPN: Ghwair 1, Tel Tif'dan (Wadi Fidan 01), Wadi Faynan 16 (WF16); PN: Wadi Fidan 51 (WFD51), Wadi Fidan 61 (WFD61), Tell Wadi Feinan.

2. Environmental and geological setting

Although today the Faynan region is part of the southern Levant's Saharo-Arabian desert zone with only ca. 60 mm annual average rainfall in the wadi valleys (Danin 1983; Rabb'a 1994), there is evidence that during the Neolithic period a wetter semi-arid environment prevailed.

Palynological and freshwater mollusc data from the Wadi Faynan catchment indicate a type of Mediterranean forest with oak, juniper, pine, olive, cypress and elm; average annual rainfall of ca. 200 mm; and meandering streams with associated riparian vegetation before ca. 8000 years ago (Hunt et al. 2004, 2007). Springs fed by groundwater and supporting riparian vegetation in gorges may have existed throughout the Holocene and would have helped mitigate the stress of variations in precipitation and mid-Holocene short-term desiccation events on human settlement (Hunt et al. 2007). Neolithic farming and herding may have played a role in vegetational degradation and alluviation such that by the Chalcolithic period the area was "virtually treeless" (Hunt et al. 2004: 928), though overgrazing may not have been significant in the Wadi Fidan until the PN or later (Twiss 2007).

Wadi Fidan 61 is located at the more arid western end of the Faynan catchment, between granitic outcrops at the mouth of the Wadi Fidan where it empties into the Wadi Arabah. Basement igneous rocks that outcrop in this area comprise the Aqaba and Arabah Complexes including the As Sadra Granodiorite Unit, the Hunayk Granodiorite Unit, the Minshar Monzogranite Unit, the Faynan Granitic Suite, the Ahaymir Volcanic Suite, and the Ghuwayr Volcanic Suite (Al-Shorman 2009: 16-18). Sedimentary rocks are exposed in some places; these include the Salib Arkosic Sandstone Formation, the Burj Dolomite-Shale Formation, the Umm Ishrin Sandstone Formation, the Kurnub Sandstone Group, the Na'ur Limestone Formation, the Fuhays-Hummar-Shuayb Formation (greenish-gray marl), and the Umm Rijam Chert-Limestone Formation (Al-Shorman 2009: 18-22) (Fig. 2). Siltstone forms thin beds in the Umm Ishrin Sandstone, Kurnub Sandstone, and Na'ur Limestone rock sequences. Superficial Pleistocene conglomerate and sediments and Holocene alluvial and aeolian deposits occur along the wadi channels. Alluvium reflects the geology of the surrounding source area, consisting of fine to coarse grained sand, granules of quartz, and granules, cobbles and boulders of limestone and basement igneous rocks.

Al-Shorman (2009: 22-24) notes possible sources of raw materials for ceramic manufacture in the Faynan area. Clay deposits are present in the upper part of the Kurnub Sandstone and lower part of the Na'ur Limestone. Marl, a calcium carbonate-rich mud or mudstone containing variable amounts of clays and silt, is available in the Na'ur Limestone, and the Fuhays-Hummer-Shuayb Formations. Erosion of these sedimentary units and weathering of granitic rocks in the area followed by re-deposition in shallow basins in wadi channels could have provided a readily available source of raw materials for pottery production. Clay minerals have been identified in the Late Pleistocene carbonate-rich fine sand and silt sediments (formerly attributed to the Lisan Marl Formation by Rabb'a 1994) that occur in parts of the western end of the drainage, near springs, and also ca. 4 km south of Wadi Fidan 61 (Al-Shdaifat et al. 2016).

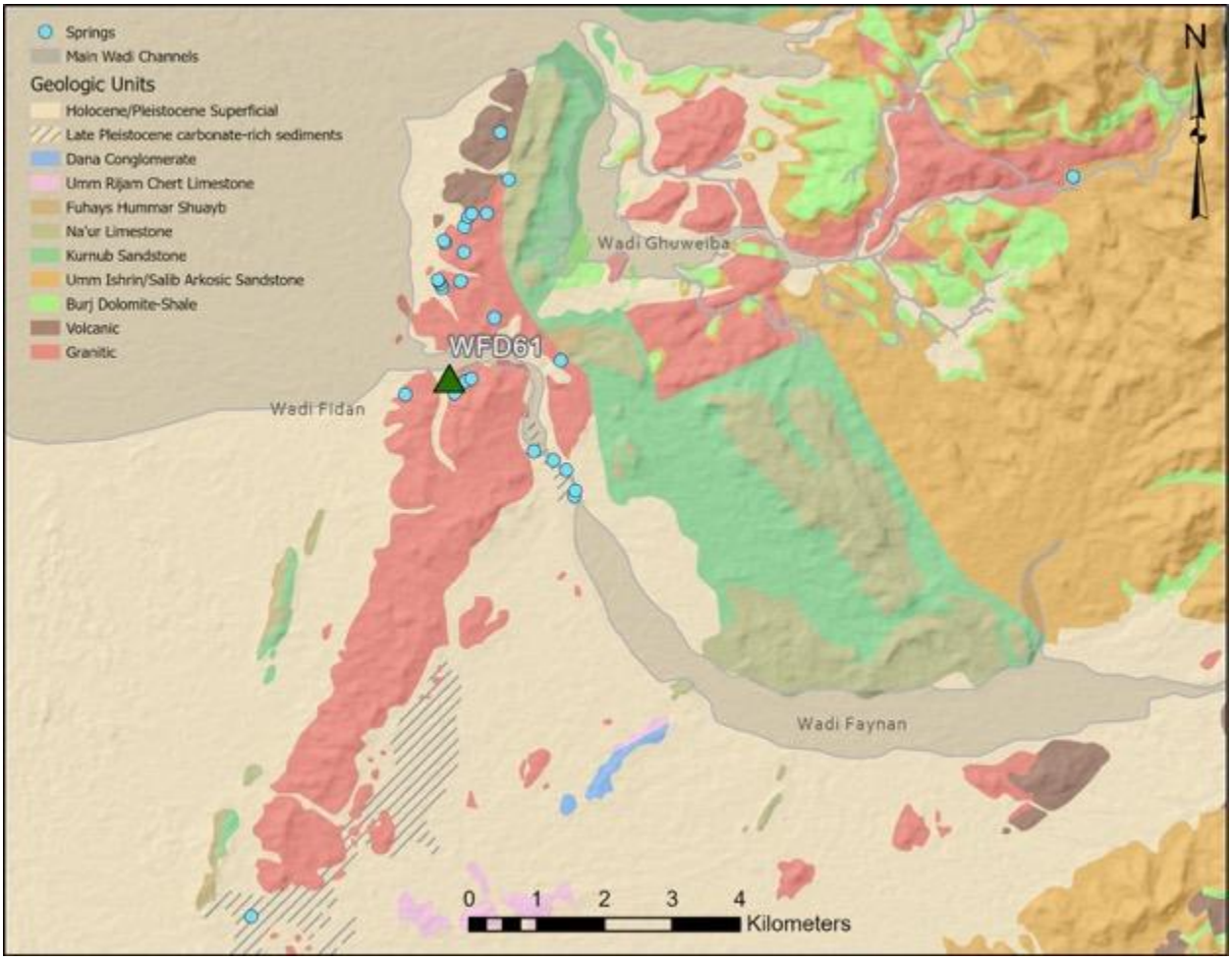

Figure 2. Simplified geological map of the Faynan study area (after Al-Shdaifat et al. 2016; Al-Shorman 2009; Rabb'a 1994).

3. Wadi Fidan 61 and its pottery assemblage

Wadi Fidan 61 is located at the confluence of the secondary Wadi al-Min B'tah and the southern bank of the main Wadi Fidan drainage (Fig. 3; Howland et al. 2014) on a monzogranite outcrop that extends over 6 ha. Portions of the area with distinct archaeological remains comprise ca. 3 ha. Juncaceae stands (rushes) growing to the east of the site indicate an oasis habitat (Cordova et al. 2013), now ephemeral springs. Based on the 1998 survey (Levy et al. 2001), it is possible that the site extended as far as the spring.

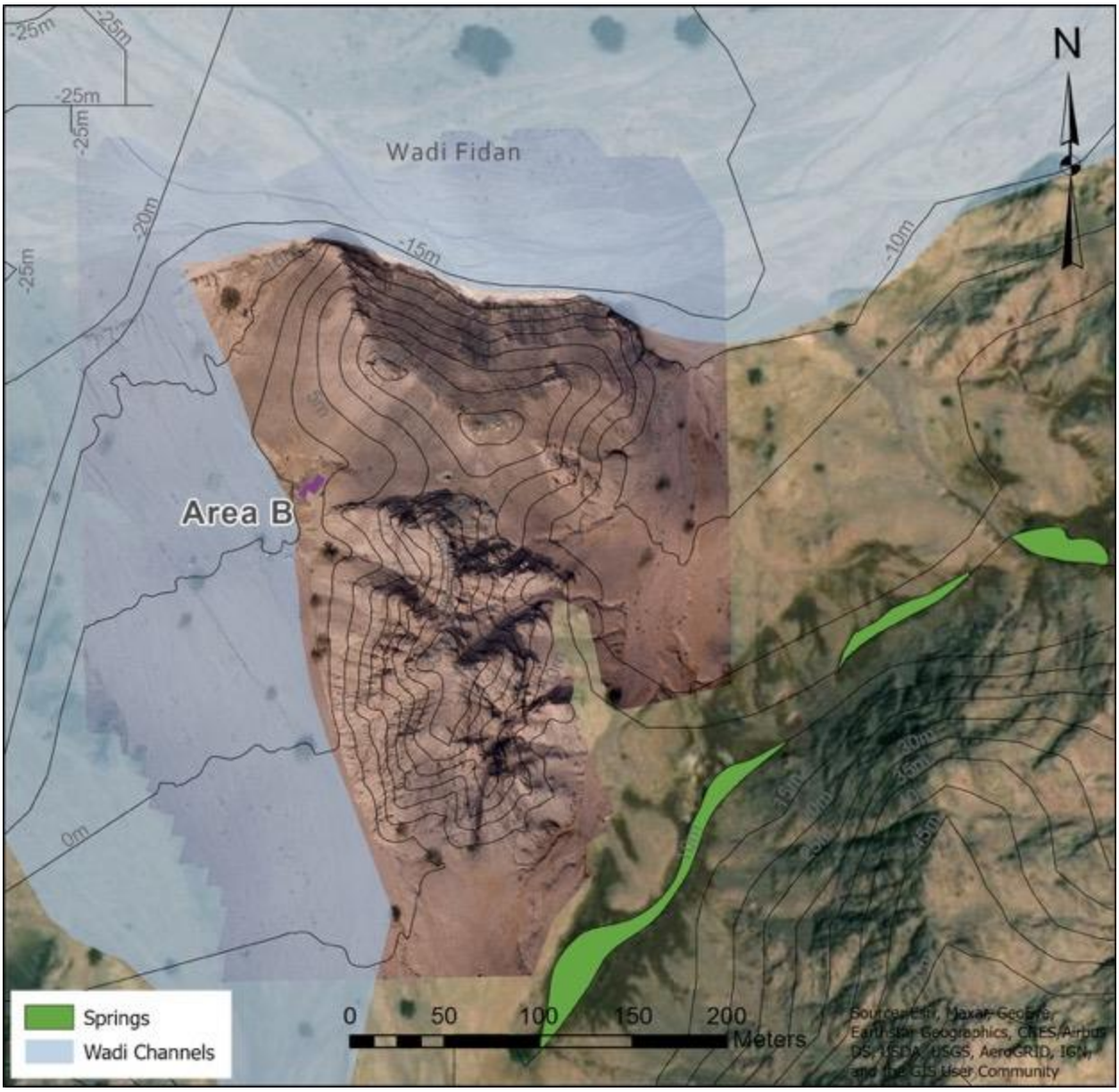

Figure 3. Contour map of Wadi Fidan 61 showing the 2012 excavation Area B.

A previously unpublished test excavation at Wadi Fidan 61 was conducted as part of the ELRAP project in 2012. A 7 x 7 m square designated Area B was opened on a natural terrace area 40 m to the north and in parallel with a small probe excavated in the 1990s that had revealed well-preserved architecture near the secondary wadi (Fig. 3). The 2012 excavation unearthed stone walls, ceramics, and an exceptionally rich archaeobotanical assemblage (Farahani 2020) relating to four occupation strata (IV-I). Lithics and faunal remains were also present. Two structures were exposed that continued in use until Stratum II (Figs. 4, 5). Structure 1, represented by one corner, was a rectilinear building constructed of large, loaf-shaped wadi cobbles laid in two rows). Structure 1 contained a circular or semi-circular installation and a hearth surrounded by thick layers of ash. Ground stone mortars and pounders were found within

and around Structure 1 as well as fragments of small circular (< 7 cm diameter) perforated chalk 'donut stones' that may represent spindle whorls. Structure 2, to the southwest and downslope from Structure 1, had one straight wall L.073, apparently built against a baulk of packed sediment, and two curved walls L.072 in the southeast and L.036 in the northwest. A hearth and ground stone artifacts were uncovered on a floor within Structure 2. One stone 'token' and one stone with incised lines were found in upper fills in Structure 2. Compact fills contained a large amount of cereal crop processing debris (Farahani 2020).

Figure 4. Overview photo of the 2012 Wadi Fidan 61 excavation. Note stone walls L.042 and L.046 forming the corner of Structure 1 with a circular or semicircular installation within (above). Structure 2 (below) is downslope from Structure 1.

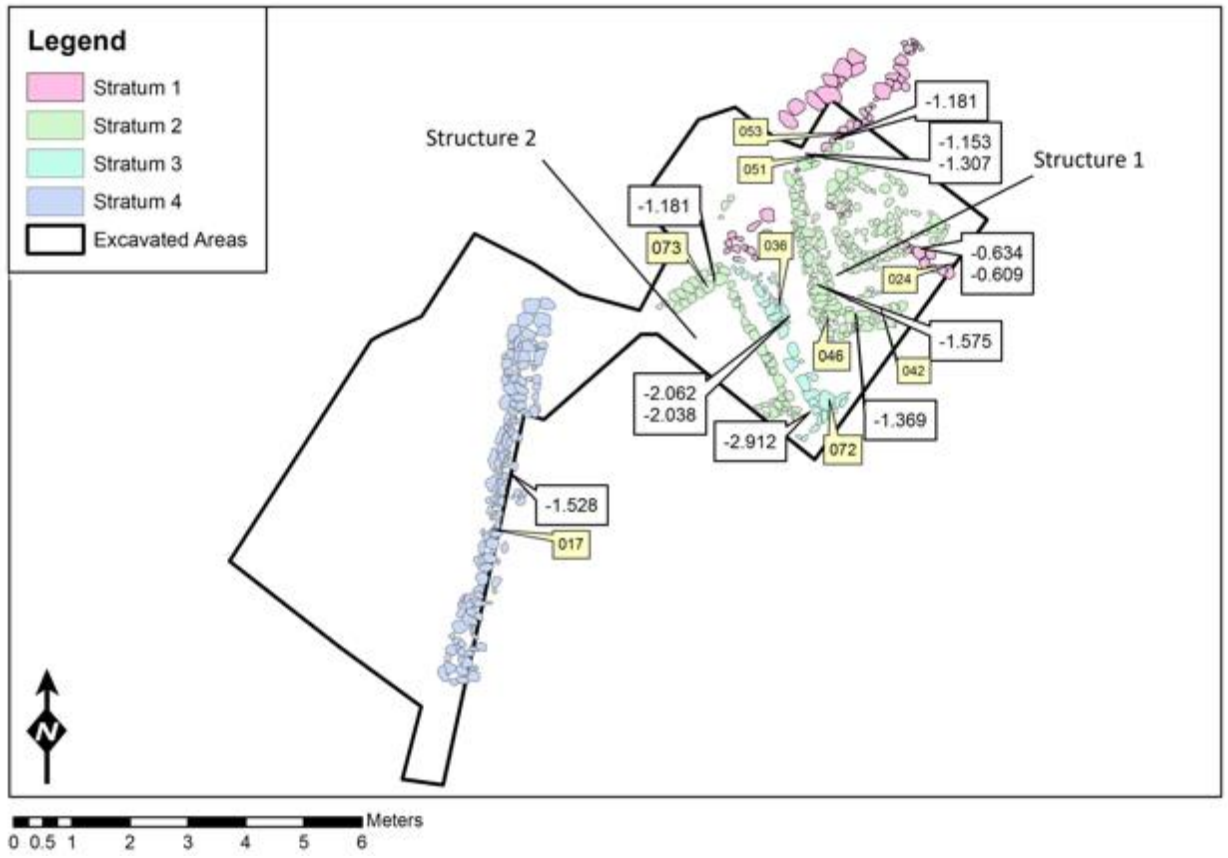

Figure 5. Wadi Fidan 61 top plan. Locus numbers are in yellow boxes. Relative elevations (m) are in white boxes.

Five radiocarbon dates from the early occupation strata (Table 1) fall within the end of the PPN and beginning of the PN possibly relating the site to the Yarmukian or Jericho IX "periods" (Banning 2018: 100, Table 6.1). Preliminary analysis of the Wadi Fidan 61 lithic assemblage supports a late Neolithic date. The assemblage includes deeply denticulated, backed sickle blades, which are considered diagnostic of the PN in Israel (Rosen 1982). A very small number of Herzliya and Nizzanim points were also identified. These are associated with the early part of the PN in the Mediterranean zones but continued in use throughout the PN in the desert areas (Gopher 1989, Rosen 1997).

Table 1. Wadi Fidan 61 radiocarbon dates.

Context	Stratum	Lab Number[1]	Sample Material, Species[2]	Uncalibrated Date B.P.	Date Cal B.C. (IntCal20, 2σ)[3]
Locus 054, Basket 30185, Ash lens in Structure 2 section	III	AA102549	Charcoal, *Pistacia atlantica*[4]	7517 +/- 66	6465- 6237
Locus 076, Basket 30293, Pit[5]	IV	AA102551	Charcoal, *Acacia* sp.	6881 +/- 51	5851-5662

Locus 044, Basket 30138, Structure 1 hearth	IV	AA102548	Charcoal, Chenopodiaceae	7288 +/- 52	6238-6054
Locus 084, Basket 30325, Structure 2 hearth	IV	AA102552	Charcoal, *Tamarix* sp.	7671 +/- 56	6601- 6429
Locus 066, Basket 30282, Structure 2 hearth	IV	AA102550	Charcoal, *Tamarix* sp.	7722 +/- 54	6645- 6461

[1]Dates processed by University of Arizona AMS dating lab.
[2]Species identification by Brita Lorentzen.
[3] Radiocarbon Calibration Program CALIB REV8.2 (Reimer *et al*. 2020; Stuiver and Reimer 1993).
[4] The older date derived from this Stratum III sample may be related to the 'old wood effect'; *Pistacia atlantica* trees can reach 1000 years old.
[5]The sample from this Stratum IV pit fill context may relate to later activity.

The Wadi Fidan 61 pottery assemblage consisted of 890 sherds recovered from all strata at the site. The pottery was highly fragmented. The assemblage included 65 diagnostic sherds, comprised of 35 rims, 19 bases, 5 handles, 3 decorated body sherds, 1 neck sherd, and 2 worked sherds. In addition to open and closed vessel forms such as bowls and jars, rim sherds possibly representing thick-walled 'spouts' and a bell-shaped form open at both ends were identified (Fig. 6). Vessel aperture diameters ranged from 8 cm to 28 cm. Bases were flat with diameters ranging from 10 to 16 cm (Fig. 7A-F). Some base sherds had mat impressions (Fig. 7D,F). Handles included ledge and pierced lugs (Fig. 7G,H). Three incised body sherds were present in the assemblage (Fig. 6G-I) as well as a rim sherd of a thumb-impressed bowl (Fig. 6A). Several sherds appeared to have a whitish wash or slip (e.g. Fig. 6A). The worked sherds (e.g. Fig. 7I) may have been tokens or spindle whorl blanks (Orrelle et al. 2012). All the pottery appeared to be handmade; a few sherds showed evidence of coil joins (Fig. 8).

The small size of the diagnostic sherds limited typological identification and formal comparisons to other possibly contemporary site assemblages. General parallels for the open and closed forms, flat bases, ledge and lug handles may be found in the Tell Wadi Feinan Neolithic assemblage (Najjar et al. 1990: 41-45, Figs. 10, 11). However, no incised decoration was noted at Tell Wadi Feinan. Similar basic shapes--handmade cups, bowls, and holemouth jars--are reported from Late Neolithic al-Basatîn (ca. 5600 B.C.E.) in the Wadi Ziqlab, northern Jordan (Kadowaki et al. 2008). Additional parallels, in particular, the thick, mat-impressed and ring bases and incised decoration, exist with Yarmukian Ware and Jericho IX Ware as described by Garfinkel (1999: 16-96) from Pottery Neolithic sites in Israel and Jordan, including Dhra' and Khirbet ed-Darih on the east side of the Dead Sea. The Wadi Fidan 61 pottery assemblage may also share generally similar typology, such as holemouth jars and bowls, and technology, such as coil-building and thick mat-impressed bases, with Late Neolithic/early Chalcolithic Qatifian pottery from the Negev and coastal plain of Israel as described by Goren (1990).

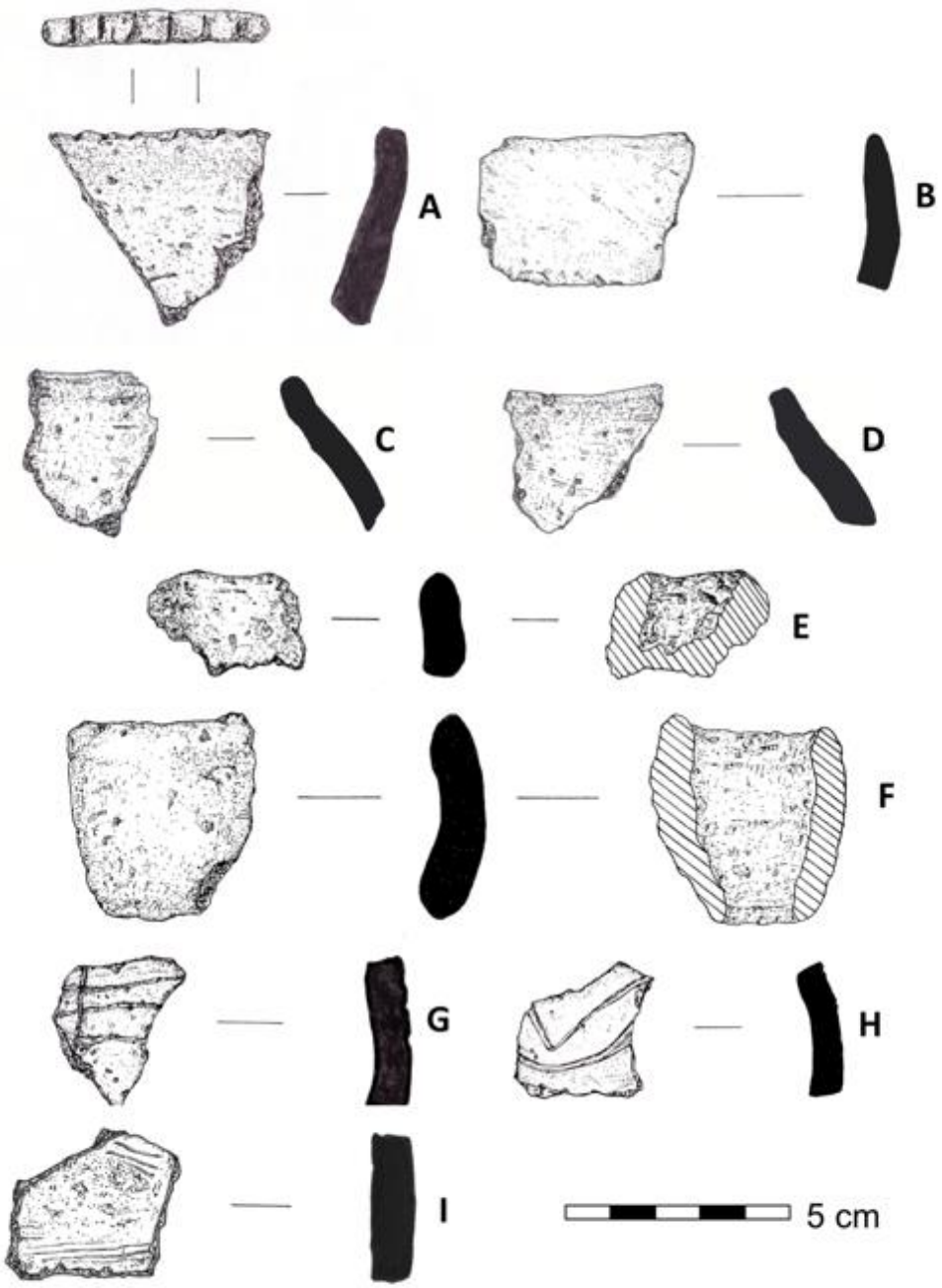

Figure 6. Examples of forms and decorated sherds in the Wadi Fidan 61 pottery assemblage. Open forms: A, bowl with impressed rim and possible whitish slip ID# 42298 (FPN029); B, straight-sided bowl ID# 42301 (FPN032). Closed forms: C, holemouth jar ID# 38552 (FPN021); D, holemouth jar ID# 42297 (FPN028). Possible 'spout': E, ID# 38314 (FPN007). Bell-shaped form: F, ID# 42300 (FPN031). Incised body sherds: G, ID# 42528 (FPN036); H, ID# 34595 (FPN038); I, ID# 32944 (FPN037). FPN numbers are analytical codes used in the compositional analysis (see Table 2).

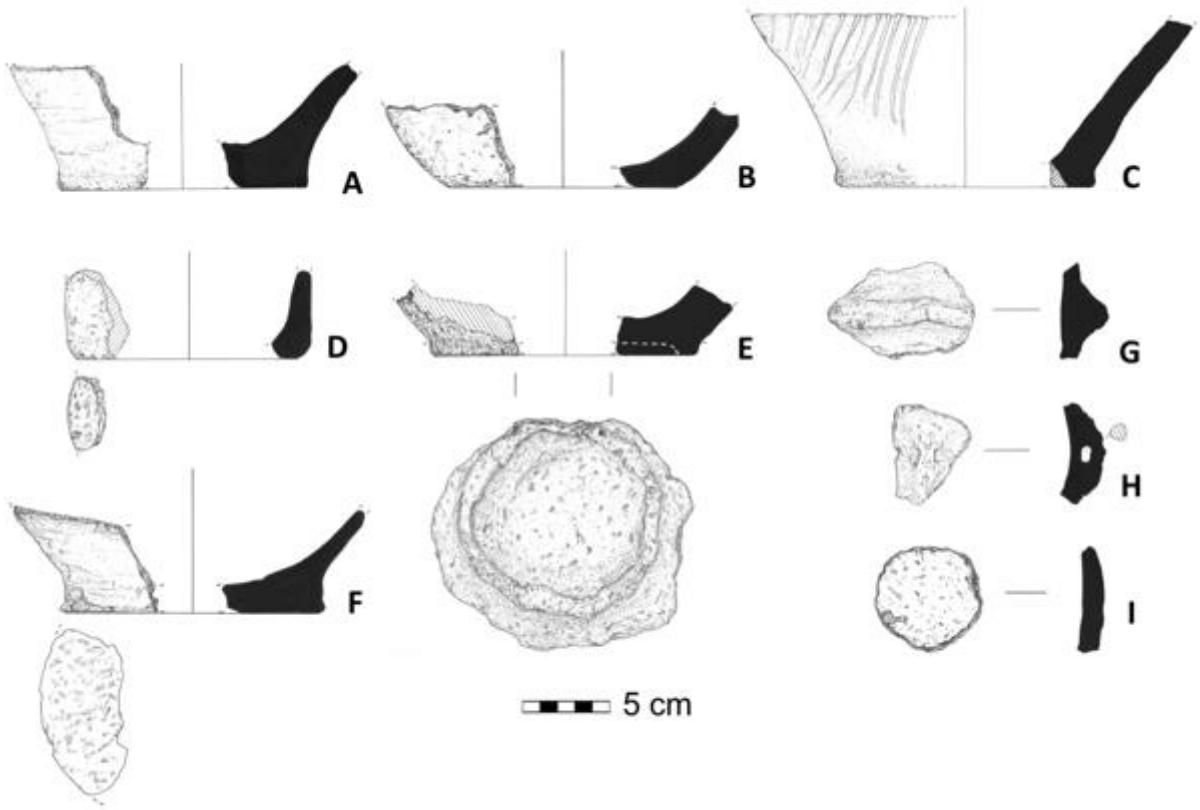

Figure 7. Examples of bases, handles and worked sherds in the Wadi Fidan 61 pottery assemblage. A, Flat base ID# 34595; B, Flat base ID# 34217; C, Flat base with diagonal faceted smoothing marks ID# 34603; D, Flat base with mat impression ID# 32614; E, Ring base ID# 32599; F, Flat base with mat impression ID# 38609; G, Ledge handle ID# 34116; H, Pierced lug handle ID# 32944; I, Worked sherd ID# 34118.

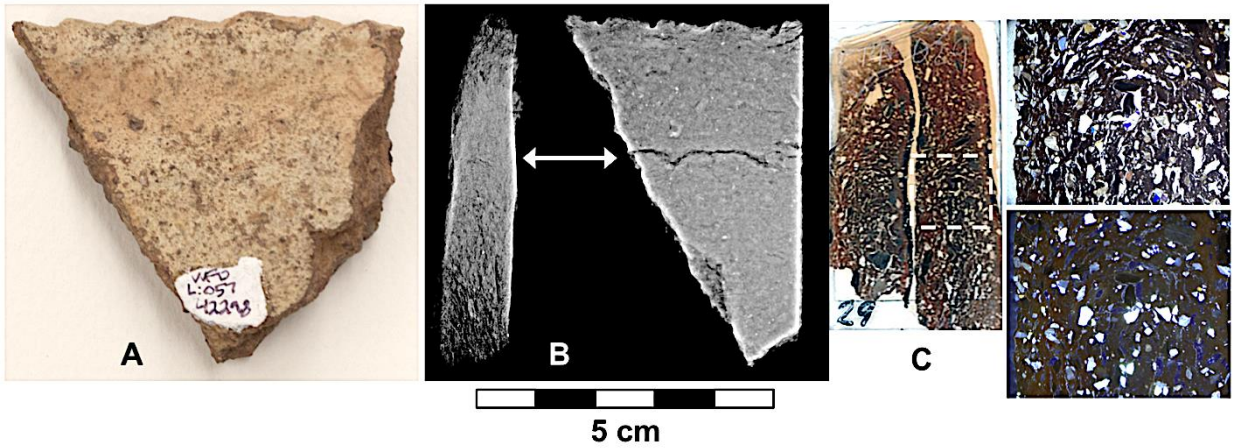

Figure 8. A, photo of interior surface of bowl rim sherd sample FPN029. B, x-radiograph of rim sherd sample FPN029 showing relic coil join in profile (left) and plan view (right). Note curve-

shaped feature in profile at level of crack in plan view. C, relic coil in thin section of rim sherd sample FPN029. Note concentric arrangement of inclusions within the magnified area (PPL, top right; XP, bottom right; image width=12 mm).

4. Methods

The sample set for the compositional study (n=38) included all rim sherds and decorated body sherds from all strata at the site (Table 2). Rim sherds were recorded as representing either open or closed vessel forms (when discernible).

Standard (30 μm) petrographic thin sections were prepared from each of the selected sherds (Quinn 2013: 23–33) and analyzed under a polarizing light microscope using a modification of the holistic, descriptive approach pioneered by Whitbread (1989, 1995). This approach considers characteristics of the clay matrix and voids in addition to the more conspicuous aplastic inclusions (Quinn 2013: 80–102). The thin sections were sorted into petrographic fabrics under the microscope without regard to vessel form type. Petrographic fabrics were then characterized by interpreting the type(s) of raw materials and steps involved in manufacture. Relationships among fabrics were also noted. Compositional, microstructural and textural criteria were used to investigate technological practices such as raw material processing, intentional addition of different types of particulate matter ('temper') and atmosphere and degree of firing (Quinn 2013: 153–203). Quantitative textural data on the size distribution of inclusions was collected for representative samples of the main fabrics. This was done by point counting evenly spaced points on the thin sections (Quinn 2013: 102-11) using a PETROG digital stepping stage and software. A minimum of 200 points and 50 measured grains were counted per sample.

Portable X-ray fluorescence spectroscopy (pXRF) was used to analyze the bulk geochemical composition of sherds. Despite concerns about the heterogeneity of coarse ware sherds (Tykot et al. 2013) and data quality from these miniaturized portable devices (Speakman and Shackley 2013), when used properly pXRF holds considerable potential for the analysis of ceramics (Holmqvist 2016; Hunt and Speakman 2015; Speakman et al. 2011). Geochemical data approaching that produced by destructive analytical techniques such as INAA is achievable if sample preparation, calibration and data quality control are optimized (Wilke 2017; Wilke et al. 2017). It remains important to acknowledge limitations of the pXRF technique in the presentation of results (Badreshany and Philip 2020).

Irradiation of the sherds was performed with an Olympus Innox-X Delta Premium hand-held device using a Rh source and a 2 mm Al filter. Analysis was undertaken at 40 kV for 120 seconds live time. Resulting spectra were deconvoluted using Bruker ARTAX software in order to correct for the individual Fe absorption/enhancement of each element, as well as for specific spectral interferences, including Rb Kß/Y Kα, Y Kß/Nb Kα and Sr Kß/Zr Kα. A Rayleigh scatter distance correction was used to compensate for the curved shape of pottery sherds. Resulting net counts were converted into concentrations via an in-house calibration for high calcium (>10% by weight) ceramics (UCL pXRF high Ca calibration 2). The in-house calibration was developed using a set of homogeneous fired clay samples spiked with four different concentrations of each of the eight oxides and elements Fe_2O_3, Ga, Nb, Rb, Sr, TiO_2, Y and Zr (32 spikes) considered to be discriminative for pottery sourcing (Wilke et al. (2017). These bespoke reference samples were prepared specifically for pXRF calibration due to the absence of natural geochemical reference materials with only one interfering element of variable concentration and the affected

elements having a fixed concentration (Wilke 2017). The spiked samples have a clay matrix that is representative for mass absorption of mid-Z elements in a broad range of clay and other aluminosilicates with a total matrix composition of elemental O, Al and Si greater than 90%. In addition to the eight spiked oxides and elements, the calibration also measured CaO, Co, Cu, K_2O, MnO, Pb and Zn, providing data on a total of 15 oxides and elements.

Two approximately 9 mm diameter circular areas (ca. 64 mm^2), representing the analytical spot size of the device, were analyzed on freshly-cut surfaces of each sherd. The results from these were averaged after calibration to account for possible heterogeneity caused by large inclusions or areas of possible clay mixing.

Performance of the Olympus Innox-X Delta Premium and the UCL pXRF calibration 2 for >10% Ca ceramics for the 15 recorded oxides and elements (CaO, Fe_2O_3, K_2O, TiO_2, Co, Cu, Ga, Mn, Nb, Pb, Rb, Sr, Y, Zn, Zr) was determined by analyzing 14 powdered certified reference materials (CRMs) of rock, ore, sediment, soil and ceramic (Appendices A, B). The CRMs were placed in a sample cup or cuvette with a 4µm prolene film, analyzed five times and calibrated using the protocol described above. The standards were also analyzed with the machine in the Soil Mode using Beam II for 120 seconds. The averages of the five measurements were compared to the certified values for the standards that fall within the range of composition found in earthenware archaeological ceramics, as determined using the data in several published geochemical studies (Quinn et al. 2010; Day et al. 2011; Trave et al. 2014; Quinn and Burton 2015), and accuracy was calculated as percentage relative difference using the formula: (measured certified)/certified) x 100 (Appendices C, D). Future geochemical studies of related ceramic material can be compared to the data collected in this study by comparison with the CRM measurements.

Selected sherds from two petrographic fabrics were analyzed under a Zeiss Evo 25 scanning electron microscope with an Oxford Instruments X-Max 80 energy-dispersive X-ray spectrometer in order to investigate microstructure and chemical composition of specific features within the ceramics. Samples were mounted in resin, polished to1µm and coated with carbon before being studied with an operating voltage of 20.0 kV and a working distance of 8.5 mm. Elemental characterization was undertaken at 1000x magnification for a live time of 20 seconds per point and an average dead-time of 40%. Multiple examples of each feature were analyzed and their average chemical composition was calculated. An in-house calibration was applied to generate normalized compositional data via stoichiometry with the Oxford Instruments AZTEC software. Data quality was monitored using two basalt standards (Hawaiian Volcano Observatory - BHVO and Columbia River - BCR-2). This indicated that Al_2O_3, CaO, Fe_2O_3, K_2O, MgO, MnO, Na_2O and SiO_2 could be measured with an accuracy of less than 3% relative error, but the data quality of P_2O and TiO_2 was poorer.

5. Results

5.1 Fabrics

Five petrographic fabrics, representing different clay 'recipes', were identified among the 38 samples (Table 2). These are described briefly here and in detail in Appendix F.

Most open and closed vessels were made from the Coarse Granitic Rock-Tempered Fabric (Fabric 1) (Fig. 9A). This fabric contains abundant poorly sorted, angular to subangular rock fragments ranging up to ca. 4 mm in size and derived mainly from granitic rocks in a non-

calcareous clay matrix with conspicuous argillaceous features (Fig. 10A). The fragments include quartz; feldspars such as plagioclase, microcline, and perthite; biotite; sometimes chert and calcite; and, rarely, volcanic and metamorphic rock. They appear to represent crushed igneous rock that was added as a temper to a non-calcareous base clay. Lumps of this clay occur in the form of laminated argillaceous inclusions of mudstone. The argillaceous inclusions suggest that the clay was collected in a dry state and prepared by crushing and hydrating mudstone, the remnants of which remain in the pottery. Crushed rock may have been added to improve the workability of the clay and/or to improve heating effectiveness or shock resistance (Müller 2016; Müller et al. 2010). However, the amounts and size of the rock grains are highly variable within the Fabric 1 samples, suggesting that the preparation and addition of temper was not strictly controlled or that the potters varied the grain size and amount of temper over time, or that the source clays, which may have been mixed, contained variable amounts of naturally occurring poorly sorted mineral inclusions.

The Argillaceous Fabric (Fabric 4) (Fig. 10D) used in the manufacture of three of the analyzed samples is related to Fabric 1 and may have been made from the same clay source, but without the addition of temper. Compared to samples of the Argillaceous Fabric (Fabric 4) (Fig. 11B, D), Fabric 1 samples have a higher proportion of mineral inclusions, a larger maximum grain size, and a lower proportion of matrix (Figs. 11A, D).

Less commonly, vessels were made of clay containing inclusions of micritic limestone, disaggregated bioclasts, microfossiliferous limestone and rare chert in a sandy, silty calcareous matrix classified here as the Calcareous Microfossiliferous Limestone Fabric (Fabric 2) (Fig. 10B). The clay source could have derived from the erosion of limestone. The inclusions, which are subangular to rounded, may be naturally occurring due to the poorly sorted grains of microfossiliferous limestone and related disaggregated bioclasts within the matrix (Fig. 11C, D). There is variation in the abundance and size of the larger limestone inclusions.

Vegetal temper was added to a similar calcareous clay source containing poorly sorted, rounded, sub-rounded and subangular sand and silt-sized inclusions of quartz and feldspar, micritic calcite and chert to produce the ceramic samples assigned to the Plant-Tempered Calcareous Fabric (Fabric 3) (Fig. 10C). These plant-tempered samples have a higher proportion of voids and lower proportion of mineral inclusions than samples of the other fabrics (Fig. 11D). The abundance of voids related to this material within the matrix of the tested sherds suggests that it was intentionally added to the clay and not incidental. The vegetal voids in three of the four samples assigned to Fabric 3 are long and curvilinear suggesting some sort of grass. The Plant-Tempered Calcareous Fabric (Fabric 3) was used for the thick-walled, possible 'spouts' (e.g. Fig. 6E). These sherds are extremely friable and their overall form and function is unclear.

The unique bell-shaped form (Fig. 6F), also with an unknown function, was manufactured from the Grog-Tempered Fabric (Fabric 5) (Fig. 9E) that has coarse inclusions of grog (up to ca. 1 mm). This was added to a base clay with variable amounts of poorly sorted silt, mainly subangular to rounded quartz, feldspar, and micritic calcite. A single sample from an open vessel was made from the Chert-Tempered Fabric (Fabric 6) (Fig. 9F). This fabric contains an abundance of angular and subangular to sub-rounded chert inclusions along with silt-sized rounded quartz and micritic calcite and rarer plagioclase and laminated mudstone inclusions. The ceramics belonging to the Chert-Tempered Fabric (Fabric 6) and the Grog-Tempered Fabric (Fabric 5) seem to have been made using the same non-calcareous base clay as the Coarse Granitic Rock-Tempered Fabric (Fabric 1) and the Argillaceous Fabric (Fabric 4) based on the presence of conspicuous argillaceous inclusions in samples belonging to all four fabrics.

Table 2. Details of Wadi Fidan 61 ceramic sherds analyzed in this report, including petrographic fabric assignment and data on geochemical composition. Fabrics: 1, Coarse Granitic Rock-Tempered Fabric; 2, Calcareous Microfossiliferous Limestone Fabric; 3, Plant-Tempered Calcareous Fabric; 4, Argillaceous Fabric; 5, Grog-Tempered Fabric; 6, Chert-Tempered Fabric. Data from those elements measured with accuracy of 20% or less are included. Major and minor elements are given as percentage weight oxides and trace elements as parts per million.

Sample	Locus/ Stratum	General Vessel Form	Fabric	Chemical Group	CaO %wt	Fe_2O_3 %wt	K_2O %wt	TiO_2 %wt	Mn ppm	Nb ppm	Rb ppm	Sr ppm	Zn ppm	Zr ppm
FPN001	5/II	Open	2	2	37.10	3.18	1.51	0.42	225	7	22	808	68	86
FPN002	12/II	Not discernible	2	2	42.75	3.06	1.53	0.48	185	8	23	868	84	94
FPN003	12/II	Open	2	2	42.53	2.95	1.91	0.45	300	7	28	848	77	119
FPN004	12/II	Not discernible	2	2	30.15	3.91	1.85	0.52	369	10	25	603	85	108
FPN005	23/II	Not discernible	1	1	5.00	4.36	2.77	0.48	444	8	75	243	37	118
FPN006	23/II	Closed	1	1	5.23	3.95	2.51	0.40	418	7	69	304	41	118
FPN007	23/II	Possible 'spout'	3	2	25.04	3.78	1.48	0.61	336	11	26	658	100	191
FPN008	23/II	Not discernible	1	1	4.44	4.40	2.85	0.45	500	7	72	271	48	120

FPN009	23/II	Possible 'spout'	3	2	28.48	3.41	1.82	0.55	271	10	27	733	83	146
FPN010	20/III	Open	1	1	2.68	5.38	2.75	0.71	352	18	92	120	42	159
FPN011	50/II	Closed	1	1	3.64	5.57	3.19	0.78	325	22	108	128	49	173
FPN012	50/II	Closed	1	1	2.99	5.73	3.86	0.83	375	12	90	240	52	185
FPN013	50/II	Closed	1	1	3.31	5.09	2.80	0.69	248	30	99	127	48	175
FPN014	68/IV	Not discernible	2	2	40.64	3.82	1.48	0.53	218	10	22	752	82	117
FPN015	26/III	Closed	1	1	10.34	4.55	2.16	0.61	530	12	72	535	53	121
FPN016	22/II	Closed	1	1	2.57	5.14	3.26	0.73	346	12	75	231	49	164
FPN017	22/II	Closed	5	1	7.10	5.77	2.22	0.75	191	11	66	307	58	137
FPN018	23/II	Open	1	1	7.18	5.08	2.42	0.64	511	10	65	247	44	120
FPN019	23/II	Closed	1	1	4.76	4.67	3.25	0.49	491	7	81	312	59	110
FPN020	23/II	Closed	4	1	1.65	5.88	2.54	0.72	169	10	57	234	49	120
FPN021	23/II	Closed	1	1	4.79	4.43	3.51	0.43	503	6	83	292	44	80

FPN022	23/II	Open	1	1	1.32	5.13	2.73	0.66	73	8	82	192	38	112
FPN023	23/II	Closed	1	1	5.60	4.95	3.28	0.52	592	8	78	325	64	101
FPN024	23/II	Closed	1	1	2.66	5.05	4.02	0.71	306	11	65	268	38	120
FPN025	23/II	Open	4	1	4.85	5.37	3.06	0.72	502	12	61	248	61	144
FPN026	32/III	Open	1	1	2.13	5.28	1.98	0.69	192	9	66	209	48	131
FPN027	23/II	Open	1	1	3.96	4.84	3.33	0.52	670	9	69	271	63	102
FPN028	23/II	Closed	1	1	2.01	5.24	2.89	0.65	173	16	96	178	41	154
FPN029	57/II	Open	1	1	3.94	5.53	2.90	0.84	406	11	81	254	46	144
FPN030	3/I	Closed	1	1	2.97	4.67	2.55	0.67	228	18	91	200	42	158
FPN031	5/II	Bell-shaped form	5	3	12.34	5.46	3.08	0.86	391	19	90	665	66	217
FPN032	35/III	Open	6	1	11.47	4.71	1.89	0.55	258	7	44	339	64	90
FPN033	20/III	Open	1	1	7.23	4.70	3.55	0.53	577	9	74	340	52	103
FPN034	12/II	Not discernible	3	2	25.35	3.24	2.05	0.59	519	9	23	513	84	185

FPN035	23/II	Possible 'spout'	3	2	27.74	3.42	1.83	0.53	259	11	29	717	82	135
FPN036	23/II	Not discernible	4	1	4.37	6.35	3.31	0.83	365	11	67	280	58	124
FPN037	38/I	Not discernible	5	3	4.62	7.20	2.39	0.86	492	11	60	768	83	136
FPN038	23/II	Not discernible	1	3	5.45	5.31	1.50	0.83	364	18	49	530	88	183

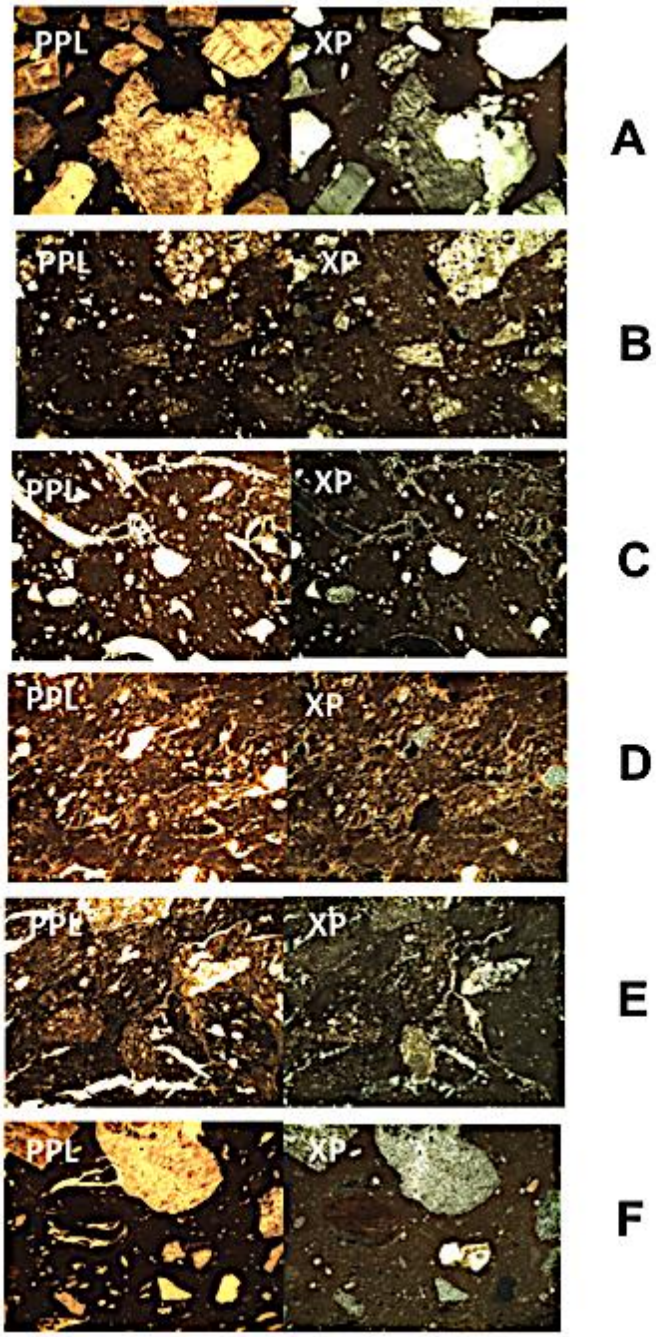

Figure 9. Photomicrographs of petrographic fabrics detected within the Wadi Fidan 61 sample set. A, Fabric 1: Coarse Granitic Rock-Tempered Fabric (FPN005) B, Fabric 2: Calcareous Microfossiliferous Limestone Fabric (FPN002). C, Fabric 3: Plant-Tempered Calcareous Fabric (FPN007). D, Fabric 4: Argillaceous Fabric (FPN020). E. Fabric 5: Grog-Tempered Fabric (FPN037). F, Fabric 6: Chert-Tempered Fabric (FPN032). Image width=3.0 mm. Images taken in plane polarized light (PPL) and crossed-polars (XP).

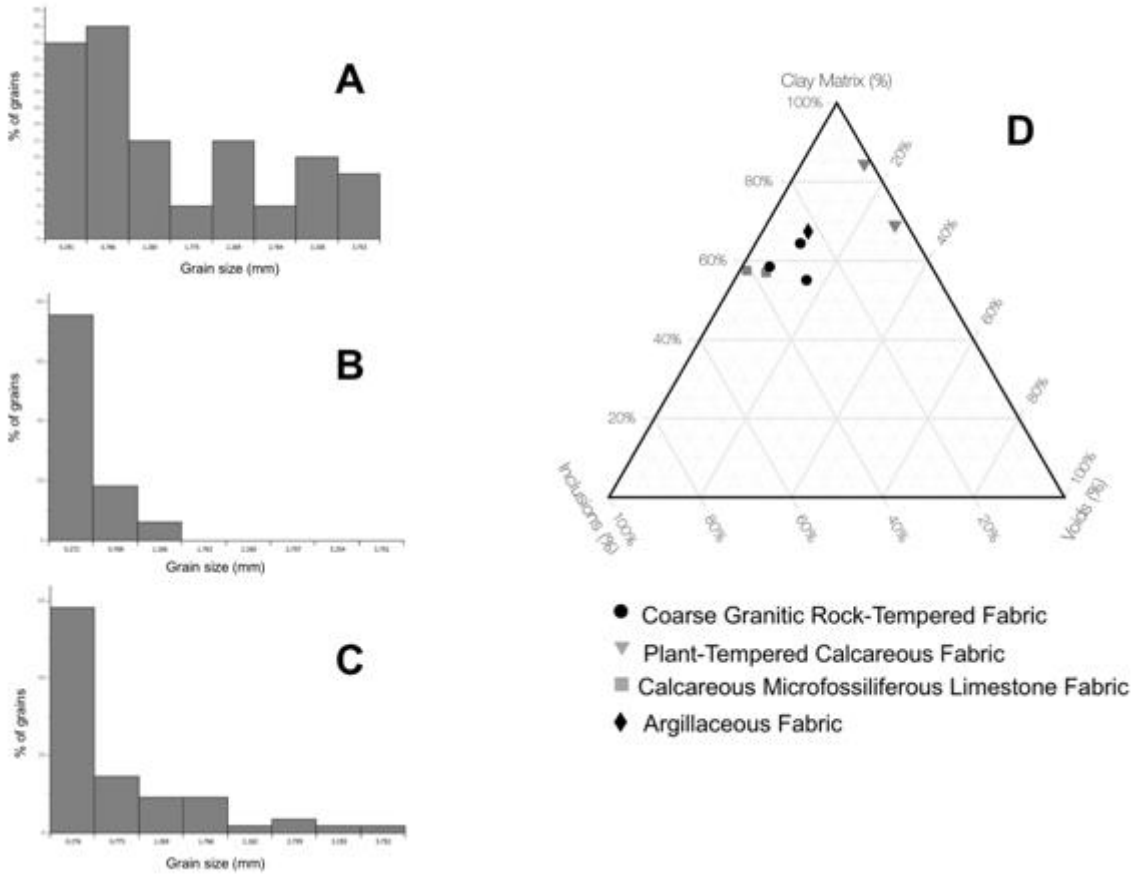

Figure 10. Quantitative textural data based on point counting for selected ceramic samples in this study. Grain size distribution histograms of inclusions: A, Grain Coarse Granitic Rock-Tempered Fabric (Fabric 1) FPN011; B, Argillaceous Fabric (Fabric 4) FPN025; C, Calcareous Microfossiliferous Fabric (Fabric 2) FPN014. D, Ternary diagram of the proportion of inclusions, clay matrix and voids within selected samples of Wadi Fidan 61 ceramic fabrics. Note that the Plant-tempered Calcareous Fabric (Fabric 3) samples have a lower proportion of inclusions and a higher proportion of voids than samples of the other fabrics. See Appendix F for point data.

5.2 Geochemical characterization and classification

Regarding performance assessment of the Olympus Innox-X Delta Premium and UCL pXRF high Ca calibration 2, the average accuracy over the standards that fall within the range of composition found in earthenware archaeological ceramics revealed that 10 of the 15 measured oxides and elements (CaO, Fe_2O_3, K_2O, TiO_2, Mn, Nb, Rb, Sr, Zn, Zr) had an average error of ≦20% relative difference between the certified and measured values (Appendix E). It should be noted that the prolene film covering the powdered CRM samples will have absorbed x-rays and could have affected the counts of some or all of the elements. Therefore, the performance of calibrations may be slightly better than determined here.

The averaged values for each of the 10 elements within the 38 ceramic sherds (Table 2) was submitted to principal components analysis (PCA) in order to explore geochemical patterning and reveal similarities and differences between samples. By plotting the first two principal components, which explained 72% of the variance in the dataset, three geochemical groups can be distinguished (Fig. 11A), based upon the abundance of several oxides and elements including CaO, Fe_2O_3, K_2O, TiO_2, Rb, Sr and Zn in the samples (Fig. 11B; Table 2). The main Chemical Group 1 is distinguished compositionally from the other two groups by its low Sr and Zn and intermediate concentration of Fe_2O_3. This group consists of samples belonging to the dominant Coarse Granitic Rock-Tempered Fabric (Fabric 1), as well as the Argillaceous Fabric (Fabric 4) and the Chert-Tempered Fabric (Fabric 6) (Fig. 11C), thus corroborating the interpretation in thin section that these share the same base clay, despite having different temper inclusions. Significant chemical variation exists within the Coarse Granitic Rock-Tempered Fabric (Fabric 1), which may reflect variation in the proportion and composition of granitic temper inclusions and their contributing elements such as K_2O and Rb.
Chemical Group 2, which contains samples from the Calcareous Microfossiliferous Limestone Fabric (Fabric 2) and the Plant-Tempered Calcareous Fabric (Fabric 3) (Fig. 11C) is characterized by high CaO, Sr and Zn and low Fe_2O_3, K_2O and Rb. While secondary calcite can be seen in thin section fringing voids and infilling pores (Cau Ontiveros et al. 2002) in sherds of most fabrics in this study (Appendix F), the high CaO and Sr of Chemical Group 2 can be explained by the occurrence of microfossiliferous limestone inclusions and/or calcareous clay matrices in these fabrics. The high proportion of CaO and corresponding lower clay content of the matrix of both fabrics is also likely to explain the low Fe_2O_3 of Chemical Group 2 relative to the other samples. Chemical Group 3, which contains two samples of the Grog-Tempered Fabric (Fabric 5) (Fig. 11C) and one sample of the Coarse Granitic Rock-Tempered Fabric (Fabric 1) is characterized by high Fe_2O_3, TiO_2, Sr and Zr; the Fe-Ti oxides and associated heavy minerals such as rutile and sphene are resistant to weathering and therefore concentrated in heavily-weathered sediments.

A comparison between the geochemical data and the shape of the ceramic vessels reveals that all closed forms plot in Chemical Group 1, while open vessel samples occur in both Chemical Groups 1 and 2 (Fig. 11D). The possible 'spouts' are restricted to Chemical Group 2 and the unique bell-shaped form plots within Chemical Group 3.

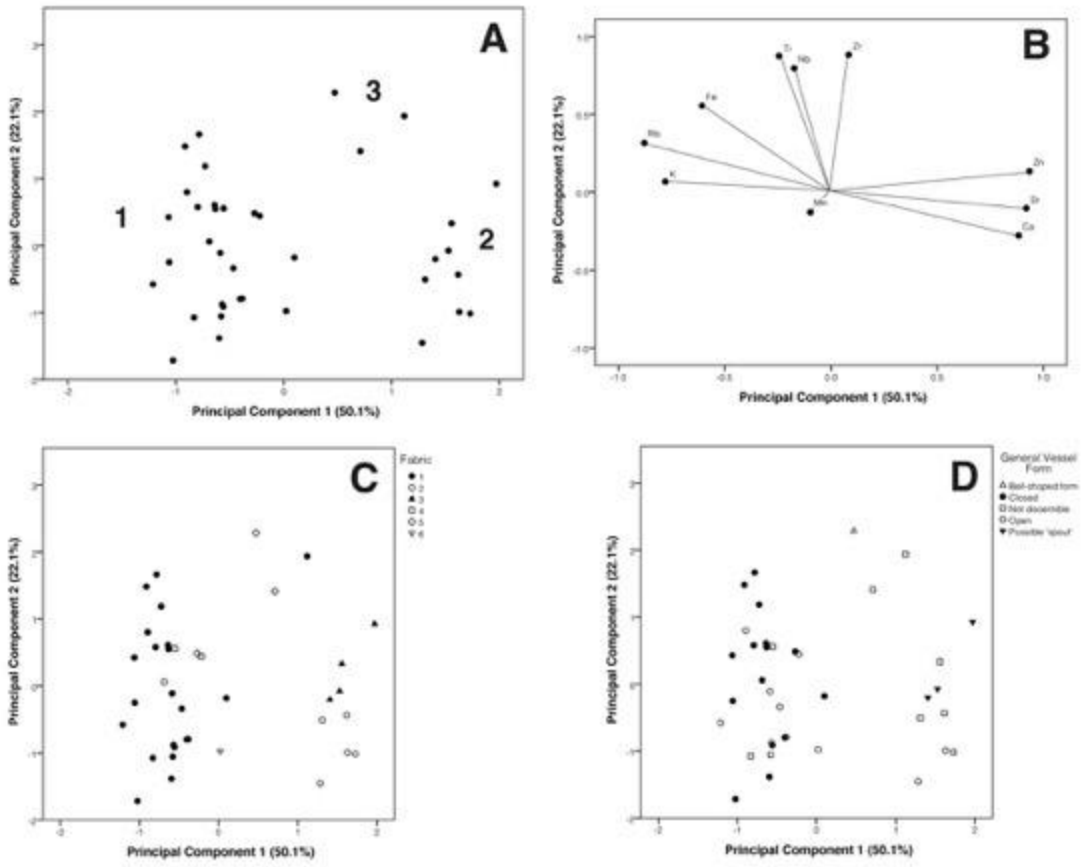

Figure 11. Statistical classification of geochemical data collected on Wadi Fidan 61 ceramic samples. A, Principal components analysis plot showing three chemical groups. B, Loading plot indicating the influence of the utilised elements on the classification, as well as their relationships with one another. C, Principal components analysis plot with samples labelled according to petrographic fabric: Fabric 1, Coarse Granitic Rock-Tempered Fabric; Fabric 2, Calcareous Microfossiliferous Limestone Fabric; Fabric 3, Plant-Tempered Calcareous Fabric; Fabric 4, Argillaceous Fabric; Fabric 5, Grog-Tempered Fabric; Fabric 6, Chert-Tempered Fabric. D, Principal components analysis plot with samples labelled according to general form.

5.3 Microstructural geochemical characterization via Scanning Electron Microscopy--Energy Dispersive X-Ray Spectroscopy (SEM-EDS)

Analysis of multiple examples of conspicuous argillaceous inclusions in sample FPN029 of the Coarse Igneous Rock-Tempered Fabric (Fabric 1) (Fig. 12A) by SEM-EDS and comparison with the surrounding clay matrix of this sample reveal that they have very similar chemical compositions (Table 3). This indicates that they are composed of the same material and confirms the interpretation in thin section that the argillaceous inclusions are poorly hydrated fragments of the clay that was used for the manufacture of the ceramics of this fabric (Quinn 2013: 171-173). The possible whitish slip layer seen on the exterior of sample FPN029 in hand specimen (Fig. 6A) is also visible in the SEM image (Fig. 12B). This is characterized by higher lime (CaO) and lower silica (SiO_2) and alumina (Al_2O_3) compared to the clay matrix of the

ceramic body to which it was applied (Table 3). The slip is likely to have been made by mixing calcareous material, such as limestone, with clay to form a light-colored slurry, which was applied to the vessel. The conspicuous grog temper inclusions in sample FPN037 of the Grog-Tempered Fabric (Fabric 5) (Fig. 12C, D) have a similar chemical composition to the surrounding base clay to which it was added (Table 3). This suggests that grog from the same pottery was added as temper, though no examples of second-generation grog (Quinn 2013: 58–59) were seen in the prepared thin section. The clay matrix of the two samples, one of Fabric 1 and one of Fabric 5, have similar chemical composition (Table 3), consistent with the statistical classification of bulk geochemical data collected on Wadi Fidan 61 ceramic samples (Fig. 11C) and supporting the interpretation that the same base clay was used in the manufacture of ceramics of both fabrics.

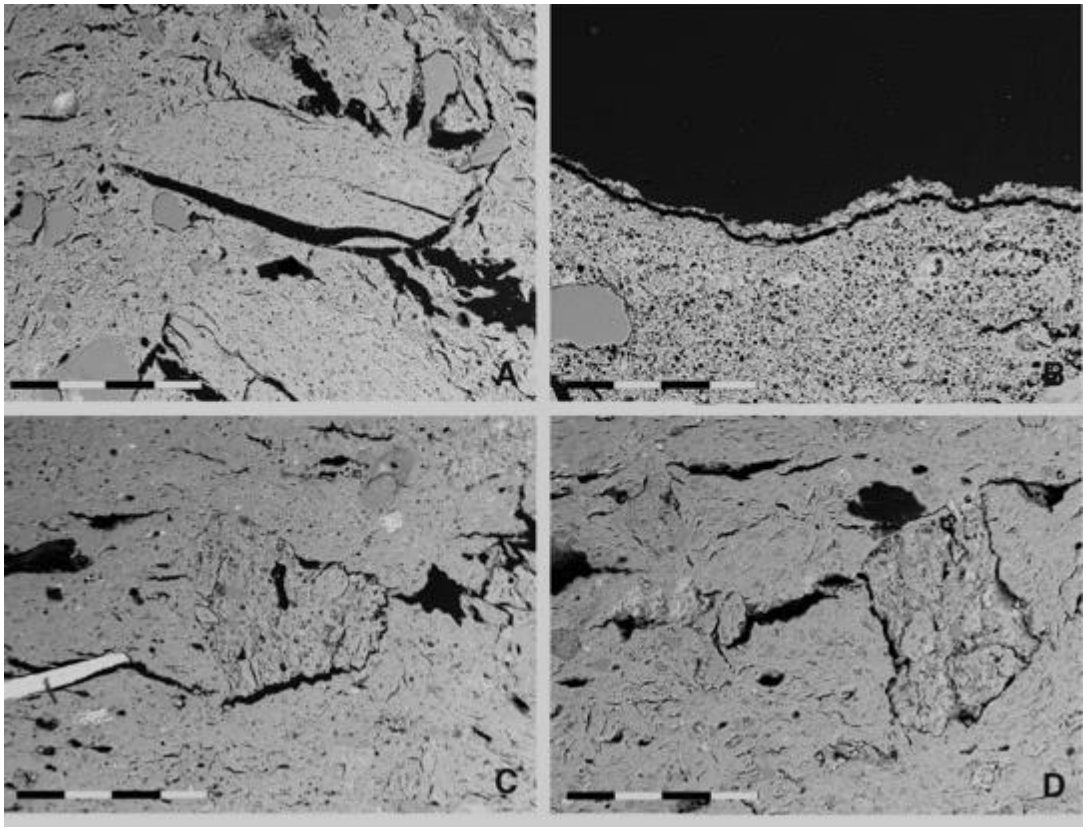

Figure 12. Back-scattered scanning electron micrographs of representative sherds from the Coarse Igneous Rock-Tempered Fabric (Fabric 1) (A and B, sample FPN029) and the Grog-Tempered Fabric (Fabric 5) (C and D, FPN037). See Table 3 for the chemical composition of selected features. Scale bar A = 1 mm. B = 0.25 mm, C = 1 mm, D = 0.5 mm.

Table 3. Geochemical characterization via SEM-EDS of selected features of representative sherds from the Coarse Igneous Rock-Tempered Fabric (FPN029) and the Grog-Tempered Fabric (FPN037). See Fig. 12 for analyzed features. Data presented as averaged normalized percentage weight oxides, from several analyses of each feature.

Sample	Feature	Na_2O	MgO	Al_2O_3	SiO_2	K_2O	CaO	TiO_2	Fe_2O_3

FPN029	Argillaceous inclusions	1.12	3.70	23.07	55.99	3.59	3.36	1.13	7.52
FPN029	Clay matrix	1.53	3.13	22.47	55.88	3.91	4.53	1.09	7.06
FPN029	Slip layer	-	1.86	3.24	11.29	0.59	79.04	-	1.28
FPN037	Clay matrix	0.26	4.15	22.39	54.83	3.31	4.90	1.07	8.61
FPN037	Grog inclusions	0.29	3.70	21.14	57.61	2.76	4.81	1.06	8.20

6. Discussion

The petrographic composition of the ceramic samples in this study includes materials derived from granitic rock and limestone. Most of the igneous rock fragments in the Coarse Granitic Rock-Tempered Fabric (Fabric 1) and the Grog-Tempered Fabric (Fabric 5) are plutonic in origin; the site is located on a granitic outcrop (Fig. 2). Rarer volcanic inclusions may have their source in the volcanic formations to the east along the Wadi Faynan drainage and also north of the site. The calcareous clay used in the manufacture of the Calcareous Microfossiliferous Limestone Fabric (Fabric 2) and the Plant-Tempered Calcareous Fabric (Fabric 3) may originate in Late Pleistocene carbonate-rich sandy clay sediments (Al-Shdaifat et al. 2016) and/or the Fuhays-Hummer-Shuayb deposits and/or be derived from erosion of the Umm Rijam Chert Limestone Formation and the Na'ur Limestone Formation. Mudstone, which is especially abundant as poorly-hydrated lumps of base clay in the Argillaceous Fabric (Fabric 4) the Coarse Granitic Rock-Tempered Fabric (Fabric 1), the Grog-Tempered Fabric (Fabric 5) and the Chert-Tempered Fabric (Fabric 6), may have been a component of the Burj Dolomite Shale Formation; thin beds of siltstone also occur in the Umm Ishrin Sandstone, Kurnub Sandstone, and Na'ur Limestone rock sequences. As noted by Al-Shorman (2009: 22-24), processes of erosion and weathering of these geological formations and re-deposition in low areas along the wadi channels suggest that all of these raw materials would have been present and accessible along the Wadi Fidan channel. Future collection and analysis of geological samples from the area could help to confirm utilization of such raw material sources by Neolithic potters at Wadi Fidan 61. Based on the data reported here, there is no evidence contradicting local production and consumption of pottery using a variety of clay deposits within ca. 5 km of the site.

There appear to be similarities between the Wadi Fidan 61 petrographic fabrics and descriptions of Neolithic pottery from Tell Wadi Feinan ca. 12 km east in the Wadi Faynan drainage (e.g. "sand grits", "calcite grits", "straw and calcite grits", "straw with flint grits"; Najjar et al. 1990: 41-46). Some more specific fabric comparisons can be made with previous petrographic studies conducted at other sites from later periods in the Faynan region. Wadi Fidan 61 Fabrics 1, 4, 5, and 6 may be related to the "Lower Cretaceous Shales" petrographic group identified by Smith et al. (2014) as the major local ceramic fabric at seven Iron Age sites in Faynan. The "Lower Cretaceous Shales" fabric, sourced to the Kurnub Sandstone formation, is described as coarse subrounded to subangular quartz sand and shale-rich minerals with rarer accessory minerals of feldspars, chert, sandstone, calcite and gypsum in a silty quartz matrix. However, Wadi Fidan 61 Fabrics 1, 4, 5, and 6 lack the common ferruginous inclusions identified in samples of the "Lower Cretaceous Shales" petrographic group. In addition, Wadi

Fidan 61 Fabric 1, which is tempered with coarse quartz, weathered plagioclase feldspar, biotite, as well as igneous rock fragments composed of these three minerals, may be related to the "Arkose" petrographic group identified by Goren (1996), which contains grains of arkose and temper of "fragments of granite or its component minerals (feldspar, quartz, biotite, hornblende)" in a clay similar to that of the Lower Cretaceous group. Goren (1996) attributed the "Arkose Group" to the Faynan area, partly on the basis of petrographic examination of the pottery assemblage from Early Bronze Age IV Khirbet Hamra Ifdan in the Wadi Fidan drainage. In an examination of a small number of surface finds from sites in the Wadi Fidan, Goren (1990) noted jar sherds made of silty "carbonatic" clay with "voids of vanished vegetal matter" and limestone or arkose sands and weathered feldspars. Based on these descriptions, Goren's (1990) samples may be similar to those of Wadi Fidan 61 Fabric 3.

Based on the Wadi Fidan 61 archaeobotanical assemblage, the community appears to have been engaged in the farming of cereals and likely legumes in the surrounding area, evidenced by an abundance of chaff in samples from Strata II-IV (Farahani 2020). The chaff would have been a ready source of temper for pottery-making. Organic temper added to ceramics increases porosity due to the voids left after firing (Quinn 2013: 219), increasing permeability and thermal insulation as well as decreasing the weight of the material. If the sherds assigned to the Plant-Tempered Calcareous Fabric (Fabric 3) do represent spouts on jars, the plant temper may have been added to keep contents of the jars cool through evaporative cooling (Rice 1987: 231). However, it is currently unknown whether these pottery fragments were attached to vessels or instead represent some other kind of ceramic objects.

Vessels appear to have been constructed by building coils onto flat disk bases that were often set on mats. The sherds were mainly fired in an oxidizing atmosphere below the vitrification level of the clay minerals (<850°C) and the degradation temperature of calcite (650–750°C; Cultrone et al. 2001) (Appendix F). Some samples have dark cores indicating a short firing duration, probably in an open bonfire or pit. These characteristics, along with the petrographic evidence for local manufacture and consumption and variation in clay sources and preparation, are consistent with an incipient ceramic technology and domestic mode of production (Rice 1987: 184).

All of the identified fabrics except for Fabric 6 are represented within the analyzed pottery samples from Stratum II which comprise the majority of the sample set (Table 3). Therefore, it seems likely that distinctly different clay deposits, some calcareous and some non-calcareous, were utilized contemporaneously. Potters may use different clay recipes depending on vessel form, size, and function (e.g. Rice 1987: 226-232); the possible 'spouts' (Fabric 3) and 'bell-shaped form' (Fabric 5) may be examples of this kind of selectivity. A compositionally diverse site assemblage may also suggest the coming together of several different social groups at the site, each of which used different clay deposits for pottery-making. However, this explanation would be better supported if some of the raw materials were identified as "non-local" (e.g. Quinn and Burton 2015; Quinn et al. 2010). Another interpretation may be that clays were collected by the same social group from different locations within a 'home range' or landscape, perhaps coincident with other tasks or activities (e.g. Michelaki et al. 2014). Notably, although the Wadi Fidan 61 community appears to have been committed to some form of cereal farming through time, a degree of foraging for wild foods is also probable given that, in addition to domesticated wheat and barley, the archaeobotanical assemblage (Farahani 2020) evidences arboreal or shrub plants that were not domesticated until two millennia after the occupation of Wadi Fidan 61, such as carob and fig (Zohary et al. 2012). The preferred environmental zones of

the wild plants present in the assemblage are varied. Carob and fig are typical of Mediterranean environments, as is *Pistacia atlantica* (Zohary 1973: 135). In contrast, date palms and colocynths, also present in the assemblage, prefer dry, sandy soils and low-humidity environments. The presence of a few specimens from the sedge family among the wild/weed seeds indicates some interaction with a partially wet environment such as springs near the site or another nearby riparian corridor. The co-occurrence of these remains suggests that the Wadi Fidan 61 community must have foraged for these plant foods over a range where all of these taxa were encounterable, so that this population might be characterized as 'farmer-foragers' (cf. Smith 2001). Springs extend north from the site along the interface of granitic, volcanic, and limestone formations as well as in the wadi channel to the southeast where Late Pleistocene carbonate-rich sands and clay sediments can be found (Al-Shdaifat et al. 2016) (Fig. 2). Plant foraging expeditions along these riparian corridors within 5 km of the site would have provided opportunities for the gathering of both calcareous and non-calcareous base clays as well as granitic rock for temper.

6. Conclusions

There are few published reports of excavated Pottery Neolithic sites and pottery from the Faynan region, which in later periods became a center of industrial-scale copper metallurgical production. Excavations at Wadi Fidan 61, dated from ca. 6500 B.C.E., revealed rectilinear stone architecture, rich archaeobotanical remains, and some of the earliest pottery in the region. As presented in this paper, thin section petrography, instrumental geochemistry and Scanning Electron Microscopy-Energy Dispersive X-Ray Spectroscopy (SEM-EDS) along with macroscopic examination were employed in a combined manner to provide complementary data for understanding how ceramic raw materials were procured, prepared and deployed for pottery-making. The results evidenced six distinct clay recipes, four of which involved the use of temper, and suggest that the pottery was manufactured from raw materials that were available near the Wadi Fidan gorge and nearby Wadi Fidan catchment area. The six petrographically-defined fabrics corresponded well with three chemical groups. A domestic mode of production is indicated by the local fabrics, the simple vessel shapes including bowls and jars, and technology including coiling and low-temperature and variable firing. The Wadi Fidan 61 fabrics, forms and manufacture methods may have some parallels with Neolithic pottery from Tell Wadi Feinan (Najjar et al. 1990: 41-46) to the east in the Faynan drainage. General vessel shapes, forming methods, and incised decoration also have parallels more broadly with Yarmukian-Jericho IX and possibly Qatifian assemblages from Israel and Jordan (Garfinkel 1999: 16-96; Garfinkel et al. 2002; Goren 1990) and Late Neolithic assemblages from northern Jordan (Kadowaki et al. 2008). Possible spindle whorl blanks suggest textile production (Orelle et al. 2012). However, the 'bell-shaped form' and the plant-tempered possible 'spouts' at Wadi Fidan 61 currently have no published parallels. The Wadi Fidan 61 archaeobotanical assemblage, evidencing a kind of farmer-forager community, provides important context for this early phase of ceramic production in the region. The procurement of different types of raw materials for pottery-making, such as calcareous and non-calcareous clay sources and granitic rock for temper, may have coincided with the collection of different types of wild plant foods sourced from a range of environmental zones, such as carob and fig from wetter Mediterranean environments, date palms and colocynths from sandy, low-humidity environments, and sedge from riparian environments near springs. By considering that resources for different tasks may have been co-located (Michelaki et

al. 2014), the technologies of subsistence and ceramics can be understood as linked and embedded within the Faynan landscape. Further, the suggested heterogeneous "taskscape" (Michelaki et al. 2014) indicates a certain degree of group mobility that may have been a strategy to cope with a trend toward aridification that intensified after ca. 8000 years ago (Fujii 2020). Studies of ceramic composition at other Pottery Neolithic sites in southern Jordan and neighboring areas may help, in future, to evaluate interpretations of the results reported here and to delineate networks of socio-economic interaction.

Acknowledgements

We thank the Department of Antiquities of Jordan for support of the Wadi Fidan 61 project. Drs. Barbara Porter and Christopher Tuttle of the American Center for Oriental Research (ACOR) in Amman also provided assistance and logistical support. Special thanks to ELRAP staff members James Darling and Aaron Gidding in the field and to the ELRAP students and volunteers in the field and the lab. Dr. Brita Lorentzen conducted species identification of the radiocarbon samples, Lindsay Harrington assisted with macroscopic examination and recording of the Wadi Fidan 61 pottery at UC San Diego, and sherd photography was done by Tyler Tucker under the supervision of Matthew Howland at UC San Diego; we appreciate their help. We also thank Tom Gregory, Technician in Scanning Electron Microscopy and X-ray Microanalysis at the Institute for Archaeology, University College London, for support and guidance in the Analytical Lab. Dr. Gilad Shtienberg provided insight regarding the geological context of Wadi Fidan 61. All scientific specimens analyzed in this study are stored at the Department of Anthropology, University of California San Diego and may be accessed by contacting the lead author. Photomicrographs and corresponding metadata for all samples in this study may be found at http://suave-dev.sdsc.edu/main/file=mburton_Wadi_Fidan_61_Pottery_Neolithic.csv&views=1110101&view=grid).

Funding

Funding for the Wadi Fidan 61 field work was awarded to TEL by the National Geographic Society Committee on Research, the C. Paul Johnson Family Foundation, the Norma and Ruben Kershaw Family Foundation, the Jerome and Miriam Katzen Family Foundation and the University of California San Diego Committee on Research. The Center for Cyber-Archaeology and Sustainability at the Qualcomm Institute, UC San Diego, and the Norma Kershaw Chair in the Archaeology of Ancient Israel and Neighboring Lands, UC San Diego, provided funding for petrography and illustration.

Declaration of Interest Statement

The authors confirm that there are no relevant financial or non-financial competing interests to report.

References

Al-Shdaifat, A., Al-Saqarat, B., and Abbas, M.
2016 An ancient wetland in the presently arid region of southern Jordan: a sedimentological and paleoenvironmental study. *Research Journal of Environmental and Earth Sciences* 8(2): 13-24. DOI:10.19026/rjees.8.2862

Badreshany, K. and Philip, G.
2020 Ceramic studies and petrographic analysis in Levantine archaeology, the limitations of current approaches. *Levant*. DOI: 10.1080/00758914.2020.1786270

Banning, E.B.
2019 It's a Small World - Work, Family Life, and Community in the Late Neolithic. Pp. 98-121 in *The Social Archaeology of the Levant - From Prehistory to the Present*, eds. Yasur-Landau, A., Cline, E. H., and Rowan, Y. M. Cambridge: Cambridge University Press.

Barker, G., Gilbertson, D., and Mattingly, D. (eds.)
2007 *Archaeology and Desertification - The Wadi Faynan Landscape Survey, Southern Jordan*. Oxford: Council for British Research in the Levant and Oxbow Books.

Cau Ontiveros, M. A., Day, P. M., and Montana, G.
2002 Secondary calcite in archaeological ceramics: evaluation of alteration and contamination processes by thin section study. Pp. 9-18 in *Modern Trends in Ancient Ceramics*, eds. Kilikoglou, V., Hein, A., and Maniatis, Y. British Archaeological Reports, International Series 1011. Oxford: Archaeopress.

Cordova, C. E., Nowell, A., Bisson, M., Ames, C. J. H., Pokines, J., Chang, M., and al-Nahar, M.
2013 Interglacial and glacial desert refugia and the Middle Paleolithic of the Azraq Oasis, Jordan. *Quaternary International* 300: 94-110. https://doi.org/10.1016/j.quaint.2012.09.019.

Cultrone, G., Rodríguez-Navarro, C., Sebastián, E., Cazalla, O. and De la Torre, M. J.
2001 Carbonate and silicate phase reactings during ceramic firing. *European Journal of Mineralogy* 13: 621–34.

Danin, A.
1983 *Desert Vegetation of Israel and Sinai*. Jerusalem: Cana.

Day, P. M., Quinn, P. S., Kilikoglou, V. and Rutter, J. A.
2011 World of Goods: Transport Jars and Commodity Exchange at the Late Bronze Age Harbor of Kommos, Crete. *Hesperia* 80: 511–58.

Farahani, A.
2020 *Analysis of Wadi Fidan 61 Archaeobotanical Assemblage*. Report on file. UC San Diego Levantine and Cyber-Archaeology Laboratory.

Finlayson, B., and S. Mithen (eds.)
2007 *The Early Prehistory of Wadi Faynan, Southern Jordan - Archaeological Survey of the Wadis Faynan, Ghuwayr and al-Bustan and evaluation of the Pre-Pottery Neolithic A site of WF 16*. Wadi Faynan Series Volume 1. Levant Supplementary Series Volume 4. Oxford: Oxbow Books.

Finlayson, B., Mithen, S. J., Najjar, M., Smith, S., Maricevic, D., Pankhurst, N., and Yeomans, L.
2011 Architecture, sedentism, and social complexity at Pre-Pottery Neolithic A WF16, Southern Jordan. *Proceedings of the National Academy of Sciences* 108(20): 8183-88.

Fujii, S.
2020 Pastoral Nomadization in the Neolithic Near East: Review from the Viewpoint of Social Resilience. Pp. 65-83 in *Resilience and Human History: Multidisciplinary Approaches and Challenges for a Sustainable Future*, eds. Nara, Y. and Inamura, T. Translational Systems Sciences 23. Singapore: Springer. DOI: 10.1007/978-981-15-4091-2_5

Garfinkel, Y.
1999 *Neolithic and Chalcolithic Pottery of the Southern Levant*. Qedem 39. Jerusalem: Institute of Archaeology, Hebrew University.

Garfinkel, Y., Miller, M. A., and Ben-Shlomo, D.
2002 *Sha'ar Hagolan*. Oxford: Oxbow Books.

Gopher, A.
1989 Neolithic Arrowheads of the Levant: Results and Implications of a Seriation Analysis. *Paléorient* 15 (1):43-56. DOI: 10.3406/paleo.1989.4484

Gopher, A.
2012 *Village communities of the Pottery Neolithic period in the Menashe Hills, Israel: archaeological investigations at the sites of Naḥal Zehora*. Emery and Claire Yass Publications in Archaeology Vol. 29. Tel Aviv: Institute of Archaeology, Tel Aviv University.

Goren, Y.
1990 The "Qatifian Culture" in Southern Israel and Transjordan: Additional Aspects for its Definition. *Mitekufat Haeven: Journal of the Israel Prehistoric Society*: 100-12.

Goren, Y.
1996 The Southern Levant in the Early Bronze Age IV: The Petrographic Perspective. *Bulletin of the American Schools of Oriental Research* 303: 33-72.

Gunneweg, J. and Balla, M.
2002 Appendix 1. Instrumental Neutron Activation Analysis, Busayra and Judah. Pp. 483-86 in *Busayra--Excavations by Crystal M. Bennett, 1971-1980*, eds. Bienkowski, P. and Balla,

M. British Academy Monographs in Archaeology No. 13. Oxford: Council for British Research in the Levant by Oxford University Press.

Hauptmann, A. and Weisgerber, G.
1987 Archaeometallurgical and mining-archaeological investigations in the area of Feinan, Wadi 'Arabah (Jordan). *Annual of the Department of Antiquities of Jordan* XXXI: 419-37.

Holmqvist, E.
2016 Handheld Portable Energy-Dispersive X-Ray Fluorescence Spectrometry (pXRF). Pp. 363-81 in *The Oxford Handbook of Archaeological Ceramic Analysis*, ed. Hunt, A. Oxford: Oxford University Press.

Howland, M. D., Kuester, F., and Levy, T. E.
2014 Photogrammetry in the Field: Documenting, Recording, and Presenting Archaeology. *Mediterranean Archaeology and Archaeometry* 14(4): 101-8.

Hunt, C., Elrishi, H. A., Gilbertson, D. D., Grattan, J. P., McLaren, S., Pyatt, B., Rushworth, G., and Barker, G.
2004 Early-Holocene environments in the Wadi Faynan, Jordan. *The Holocene* 14(6): 921-30. DOI: 10.1191/0959-683604hl769rp

Hunt, C. O., Gilbertson, D. D., and El-Rishi, H. A.
2007 An 8000-year history of landscape, climate, and copper exploitation in the Middle East: The Wadi Faynan and the Wadi Dana National Reserve in southern Jordan. *Journal of Archaeological Science* 34 (8): 1306-38. DOI: 10.1016/j.jas.2006.10.022

Kadowaki, S., Gibbs, K., Allentuck, A., Banning, E. B.
2008 Late Neolithic Settlement in Wadi Ziqlab, Jordan: Al-Basatîn. *Paléorient* 34(1): 105-129 DOI: 10.2307/41496833

Kuijt, I., and Chesson, M.
2002 Excavations at ‘Ain Waida, Jordan: New Insights into Pottery Neolithic Lifeways in the Southern Levant. *Paléorient* 28(2): 109-22.

Levy, T. E.
2007 *Journey to the Copper Age - Archaeology in the Holy Land*. San Diego: San Diego Museum of Man.

Levy, T. E., Adams, R. B., Witten, A. J., Anderson, J., Arbel, Y., Kuah, S., Moreno, J., Lo, A., and Waggoner, M.
2001 Early metallurgy, interaction, and social change: The Jabal Hamrat Fidan (Jordan) research design and 1998 archaeological survey: Preliminary report. *Annual of the Department of Antiquities of Jordan* 45: 159-87.

Levy, T.E., Najjar, M., and Ben-Yosef, E.

2014 *New Insights into the Iron Age Archaeology of Edom, Southern Jordan*. Los Angeles: Cotsen Institute of Archaeology Press.

MacDonald B.
1987 Southern Ghors and northeast 'Araba archaeological survey, 1985 and 1986. *Syria* 64: 305-8.

MacDonald, B.
1992 *The Southern Ghors and Northeast 'Arabah Archaeological Survey***.** Sheffield Archaeological Monographs 5. Sheffield: J.R. Collis Publications Department of Archaeology and Prehistory, University of Sheffield.

MacDonald, B., Clark, G. A., and Neeley, M.
1988 Southern Ghors and northeast ʿAraba archaeological survey 1985 and 1986, Jordan: A preliminary report. *Bulletin of the American Schools of Oriental Research*: 23-45.

Michelaki, K., Braun, G. V., and Hancock, G. V.
2014 Local clay sources as histories of human–landscape interactions: a ceramic taskscape perspective. *Journal of Archaeological Method and Theory* 22: 783–827.

Müller, N. S.
2016 Mechanical and thermal properties. Pp. 321–42 in *The Oxford Handbook of Archaeological Ceramic Analysis,* ed. Hunt, A. Oxford: Oxford University Press.

Müller, N. S., Kilikoglou, V., Day, P. M., and Vekinis, G.
2010 The influence of temper shape on the mechanical properties of archaeological ceramics. *Journal of the European Ceramic Society* 30: 2457–65.

Najjar, M., Abu Dayya, A., Suleiman, E., Weisgerber, G., and Hauptmann, A.
1990 Tell Wadi Feinan: The first Pottery Neolithic tell in the south of Jordan. *Annual of the Department of Antiquities of Jordan* 34: 27-56.

Orrelle, E., Eyal, R., and Gopher, A.
2012 Spindle Whorls and Their Blanks. Pp. 632-56 in *Village communities of the Pottery Neolithic period in the Menashe Hills, Israel: archaeological investigations at the sites of Naḥal Zehora*, ed. Gopher, A. Emery and Claire Yass Publications in Archaeology Vol. 29. Tel Aviv: Institute of Archaeology, Tel Aviv University.

Quinn, P. S.
2013 *Ceramic Petrography: The Interpretation of Archaeological Pottery and Related Artefacts in Thin Section*. Oxford: Archaeopress.

Quinn, P. S. and Burton, M. M.
2015 Ceramic Distribution, Migration and Cultural Interaction Among Late Prehistoric (ca. 1300–200 B.P.) Hunter-Gatherers in the San Diego Region, Southern California. *Journal of Archaeological Science Reports* 5: 285-95.

Quinn, P. S., Day, P. M. and Kilikoglou, V.
2010 Keeping an Eye on Your Pots: The Provenance of Neolithic Ceramics from Cyclops Cave on the Island of Youra, Greece. *Journal of Archaeological Science* 37: 1042-52.

Rabb'a, I.
1994 Geology of the Qurayqira (Jabal Hamra Fadan). Map sheet 3051 II. Amman: Ministry of Energy and Natural Resources Authority, Geology Directorate, Geological Mapping Division Bulletin 28.

Raikes, T. D.
1980 Notes on Some Neolithic and Later Sites in Wadi Araba and the Dead Sea Valley. *Levant* 12 (1): 40-60. DOI: 10.1179/007589180790211877.

Reimer P, Austin, W. E. N., Bard, E., Bayliss, A., Blackwell, P. G., Bronk Ramsey, C., Butzin, M., Edwards, R. L., Friedrich, M., Grootes, P. M., Guilderson, T. P., Hajdas, I., Heaton, T. J., Hogg, A., Kromer, B., Manning, S. W., Muscheler, R., Palmer, J. G., Pearson, C., van der Plicht, J., Reim Richards, D. A., Scott, E. M., Southon, J. R., Turney, C. S. M., Wacker, L., Adolphi, F., Büntgen, U., Fahrni, S., Fogtmann-Schulz, A., Friedrich, R., Köhler, P., Kudsk, S., Miyake, F., Olsen, J., Sakamoto, M., Sookdeo, A. and Talamo, S.
2020 The IntCal20 Northern Hemisphere radiocarbon age calibration curve (0-55 cal kB). *Radiocarbon* 62 (4): 725-757. DOI: 10.1017/RDC.2020.41.

Rice, P. M.
1987 *Pottery Analysis: A Sourcebook*. Chicago: The University of Chicago Press.

Rollefson, G.O.
2008 The Neolithic Period. Pp. 71-108 in *Jordan - An Archaeological Reader*, ed. Adams, R. B. London: Equinox.

Rosen, S. A.
1982 Flint Sickle-blades of the Late Protohistoric and Early Historic Periods in Israel. *Tel Aviv* 9(2): 139-45. DOI:10.1179/tav.1982.9.2.139.

Rosen, S. A.
1997 *Lithics After the Stone Age: A Handbook of Stone Tools from the Levant*. Lanham: AltaMira Press.

Simmons, A. H., and Najjar, M.
2006 Ghwair I: A Small, Complex Neolithic Community in Southern Jordan. *Journal of Field Archaeology* 31 (1): 77-95. DOI: 10.1179/009346906791072052.

Smith, B. D.
2001 Low-level food production. *Journal of Archaeological Research* 9: 1–43.

Smith, N. G., Goren, Y. and Levy, T. E.

2014 The Petrography of Iron Age Edom: From the Lowlands to the Highlands. Pp. 461-91 in *New Insights into the Iron Age Archaeology of Edom, Southern Jordan*, eds. Levy, T.E., Najjar, M., and Ben-Yosef, E. Los Angeles: Cotsen Institute of Archaeology Press.

Speakman, R. J. and Shackley, M. S.
2013 Silo Science and Portable XRF in Archaeology: A Response to Frahm. *Journal of Archaeological Science* 40: 1435-43.

Speakman, R. J., Little, N. C., Creel, D., Miller, M. R. and Iñañez, J. G.
2011 Sourcing Ceramics with portable XRF spectrometers? A Comparison with INAA using Mimbres Pottery from the American Southwest. *Journal of Archeological Science* 38: 3483-96.

Stuiver, M. and Reimer, P.J.
1993 Extended 14C data base and revised CALIB 3.0 14C age calibration program. *Radiocarbon* 35:215-230.

Twiss, K. C.
2007 The Zooarchaeology of Tel Tif'dan (Wadi Fidan 001), Southern Jordan. *Paléorient* 33(2): 127-45.

Tykot, R. H., White, N. M., Du Vernau, J. P., Freeman, J. S., Hays, C. T., Koppe, M., Hunt, C. N., Weinstein, R. A. and Woodward, D. S.
2013 Advantages and Disadvantages of pXRF for Archaeological Ceramic Analysis: Prehistoric Pottery Distribution and Trade in NW Florida. Pp. 233-44 in *Archaeological Chemistry VIII*, eds. Armitage, R. A. and Burton, J. H. Washington, D.C.: American Chemical Society.

Whitbread, I. K.
1989 A proposal for the systematic description of thin sections towards the study of ancient ceramic technology. Pp. 127-38 in *Archaeometry: Proceedings of the 25th International Symposium*, ed. Maniatis, Y. Amsterdam: Elsevier.

Whitbread, I. K.
1995 *Greek Transport Amphorae: A Petrological and Archaeological Study*. Fitch Laboratory Occasional Paper 4. Athens: British School at Athens.

Wilke, D.
2017 Some Updated Quality Concerns on Non-Destructive Geochemical Analysis with XRF Spectrometry. *Advances in Applied Science Research* 8: 90-4.

Wilke, D., Rauch, D. and Rauch, P.
2017 Is Non-destructive Provenancing of Pottery Possible with Just a Few Discriminative Trace Elements? *STAR: Science & Technology of Archaeological Research* 2(2): 141-58. DOI: 10.1080/20548923.2016.1209030.

Zohary, D., Hopf, M. and Weiss, E.
2012 *Domestication of Plants in the Old World: The origin and spread of domesticated plants in Southwest Asia, Europe, and the Mediterranean Basin*. 4th ed. Oxford: Oxford University Press.

Zohary, M.
1973 *Geobotanical foundations of the Middle East* (Geobotanica Selecta). Stuttgart: G. Fischer.

Supplementary material

Appendix A. Details of 14 certified reference materials used to assess the performance of UCL pXRF calibration 2 for >10% Ca ceramics in this paper. See Appendix B for certified values.

Code	Name
CGL 111	Rare earth ore
CGL 002	Alkaline granite
CGL 006	Nepheline syenite
CGL 007	Basalt

GBM306-12	Certified Ore Grade Base Metal
SARM 1	NIM-G Granite
SARM 41	Carbonaceous Shale
SARM 42	Soil
SARM 44	Sillimanite Schist
SARM 45	Kinzingite
SARM 48	Fluorspar Granite
SARM 50	Dolerite
SARM 52	Stream Sediment
SARM 69	Ceramic-1

Appendix B. Certified values for 13 reference materials used to assess the performance of UCL pXRF calibration 2 for >10% Ca ceramics and the manufacturer's Soil Mode calibration. Values given in percentage weight.

Standard	Ca	Co	Cu	Fe	Ga	K	Mn	Nb	Pb	Rb	Sr	Ti	Y	Zn	Zr
CGL 111	18.23000	0.00325	0.01470	9.51000		0.75500	0.10800		0.11000	0.00430	2.24000	0.09000	0.09590	0.06000	
CGL 002	0.27700		0.00070	0.35000	0.00570	2.97000		0.00640	0.00630	0.23600	0.00123	0.01740	0.00230	0.00920	0.00400
CGL 006	1.63000	0.00100	0.00260	1.83900	0.00230	7.55000	0.10840	0.00400	0.01140	0.02070	0.17400	0.22200	0.00230	0.00980	0.06000
CGL 007	3.87000	0.00360	0.00320	6.88800	0.00230	3.31000	0.10070	0.00520	0.00090	0.00630	0.09270	1.26500	0.00200	0.01140	0.02870
GBM306-12		0.00225	1.49000	3.59500					2.70950	0.07200				2.06300	
SARM 1	0.56000		0.00120	1.40000	0.00270	4.14000	0.01600			0.03250	0.00100	0.05400		0.00500	0.03000
SARM 41	1.07200	0.00150	0.00530	2.96000	0.00200	1.15400	0.04600	0.00080	0.00300	0.00590	0.00540	0.33000	0.00170	0.00760	0.01460
SARM 42	0.63600	0.00350	0.00170	3.27000	0.00120	0.37300	0.07700	0.00080	0.00100	0.00220	0.00370	0.21600	0.00110	0.00440	0.01920
SARM 44	0.10000	0.00080	0.00100	1.44000	0.00550	0.14900	0.02300	0.00960	0.00300	0.00130	0.00050	1.09700	0.00840	0.02710	0.04060
SARM 45	0.55800	0.00410	0.00110	8.81000	0.00350	2.64000	0.07700	0.00270	0.00200	0.01420	0.00920	1.09100	0.00630	0.00740	0.03220
SARM 48	6.36000		0.00100	0.41000		3.54000	0.01500	0.02020	0.01350	0.02910	0.00290	0.06000	0.04360	0.00530	0.03000

SARM 50	7.72000	0.00400	0.00840	7.96000		0.51000	0.13200	0.00100	0.00250	0.00140	0.01950	0.51600	0.00230	0.00810	0.00860
SARM 52	0.26400	0.00810	0.02190	13.78000	0.00150	0.20700	0.20900	0.00110		0.00200	0.00250	0.77900	0.00200	0.02640	0.02500
SARM 69	1.69000	0.00280	0.00460	5.02000		1.63000	0.10000	0.00090	0.00140	0.00660	0.01090	0.46600	0.00290	0.00680	0.02710

Appendix C. Comparison of certified and measured values for 14 reference materials used to assess the performance of manufacturers Soil Mode pXRF calibration. Accuracy calculated using the formula (measured-certified)/certified) x 100 and given in percentage relative error.

Standard		**Cu**	**Fe**	**Mn**	**Nb**	**Pb**	**Rb**	**Sr**	**Ti**	**Y**	**Zn**	**Zr**
CGL 111	certified	0.015	9.510	0.108		0.110	0.004	2.240		0.096	0.060	
	measured	0.008	8.686	0.382	0.001	0.077	0.002	1.644	1.282	0.081	0.049	0.014
	accuracy	-47.347	-8.660	253.852		-29.909	-52.047	-26.624		-15.704	-18.933	
CGL 002	certified	0.001	0.350		0.006	0.006	0.236	0.001	0.017	0.002	0.009	0.004
	measured	0.008	0.252	0.096	0.006	0.008	0.256	0.001	0.144	0.002	0.011	0.006
	accuracy	1041.574	-27.977		-0.158	22.984	8.602	21.626	725.402	-15.826	15.304	41.300
CGL 006	certified	0.003	1.839		0.004	0.011	0.021	0.174	0.222	0.002	0.010	0.060

	measured	0.004	1.336	0.081	0.003	0.012	0.020	0.176	0.311	0.003	0.010	0.079
	accuracy	63.576	-27.328		-16.572	6.579	-5.188	1.356	40.081	15.565	-2.714	31.833
CGL 007	certified	0.003	6.888	0.101	0.005	0.001	0.006	0.093	1.265	0.002	0.011	0.029
	measured	0.007	6.340	0.092	0.004	0.001	0.006	0.087	1.092	0.002	0.011	0.036
	accuracy	119.665	-7.962	-8.620	-14.627	4.667	-10.032	-6.516	-13.696	-1.100	-2.140	25.631
GBM306-12	certified	1.490	3.595			2.710	0.072				2.063	
	measured	2.970	5.487	2.660	0.000	2.358	0.064	0.004	1.005	0.002	2.428	0.030
	accuracy	99.333	52.629			-12.983	-10.861				17.703	
SARM 1	certified	0.001	1.400	0.016			0.033	0.001	0.054		0.005	0.030
	measured	0.006	1.086	0.014	0.005	0.004	0.033	0.001	0.140	0.015	0.006	0.039
	accuracy	374.474	-22.421	-10.625			1.926	7.600	160.111		28.600	30.167
SARM 41	certified	0.005	2.960	0.046	0.001	0.003	0.006	0.005	0.330	0.002	0.008	0.015
	measured	0.015	2.642	0.041	0.001	0.001	0.006	0.005	0.393	0.002	0.009	0.019
	accuracy	183.861	-10.730	-10.304	-4.775	-61.933	-3.729	1.519	19.230	-0.588	12.632	28.260

SARM 42	certified	0.002	3.270	0.077	0.001	0.001	0.002	0.004	0.216	0.001	0.004	0.019
	measured	0.007	2.796	0.065	0.000	0.001	0.002	0.004	0.231	0.001	0.005	0.026
	accuracy	288.747	-14.489	-15.117	-60.495	-10.000	1.455	-1.838	7.102	3.636	20.045	34.240
SARM 44	certified	0.001	1.440	0.023	0.010	0.003	0.001	0.001	1.097	0.008	0.027	0.041
	measured	0.005	1.141	0.019	0.009	0.003	0.002	0.000	0.766	0.010	0.027	0.061
	accuracy	372.031	-20.757	-18.609	-10.818	-4.533	16.462	-10.000	-30.201	13.524	0.450	49.099
SARM 45	certified	0.001	8.810	0.077	0.003	0.002	0.014	0.009	1.091	0.006	0.007	0.032
	measured	0.003	9.170	0.077	0.002	0.002	0.013	0.009	1.201	0.006	0.008	0.039
	accuracy	196.354	4.084	-0.623	-8.390	-20.200	-6.577	-7.370	10.092	2.889	12.838	22.205
SARM 48	certified	0.001	0.410	0.015	0.020	0.014	0.029	0.003	0.060	0.044	0.005	0.030
	measured	0.004	0.289	0.016	0.010	0.015	0.027	0.003	0.122	0.047	0.007	0.040
	accuracy	330.690	-29.473	8.533	-52.351	11.452	-6.014	-2.345	103.400	8.353	40.415	32.940
SARM 50	certified	0.008	7.960	0.132	0.001	0.003	0.001	0.020	0.516	0.002	0.008	0.009
	measured	0.015	7.168	0.119	0.001	0.002	0.001	0.018	0.532	0.002	0.009	0.010

	accuracy	76.316	-9.946	-10.136	-48.212	-10.320	-18.000	-7.754	3.008	-0.435	8.000	11.721
SARM 52	certified	0.022	13.780	0.209	0.001		0.002	0.003	0.779	0.002	0.026	0.025
	measured	0.030	17.950	0.264	0.001	0.097	0.002	0.002	1.324	0.002	0.023	0.032
	accuracy	34.751	30.259	26.153	-26.215		11.400	-6.400	70.021	19.700	-12.576	28.464
SARM 69	certified	0.005	5.020	0.100	0.001	0.001	0.007	0.011	0.466	0.003	0.007	0.027
	measured	0.011	4.684	0.089	0.001	0.001	0.007	0.011	0.486	0.003	0.007	0.038
	accuracy	143.252	-6.685	-10.900	-0.559	6.857	-0.788	-1.101	4.292	9.724	8.559	38.568

Appendix D. Comparison of certified and measured values for 14 reference materials used to assess the performance of UCL pXRF calibration 2 for >10% Ca ceramics. Accuracy calculated using the formula (measured-certified)/certified) x 100 and given in percentage relative error.

Standard		**Ca**	**Co**	**Cu**	**Fe**	**Ga**	**K**	**Mn**	**Nb**	**Pb**	**Rb**	**Sr**	**Ti**	**Y**	**Zn**	**Zr**
CGL 111	certified	18.230	0.003	0.015	9.510		0.755	0.108		0.110	0.004	2.240		0.096	0.060	
	measured	17.00	0.0018	0.0108	8.1810	0.00027	0.38	0.0711	0.00204	0.063	0.0072	1.4222	0.0000	0.06336	0.0361	0.0230
	accuracy	-6.748	-43.083	-26.556	-13.975		-49.423	-34.204		-42.832	67.789	-36.508		-33.926	-39.853	
CGL 002	certified	0.277		0.001	0.350	0.006	2.970		0.006	0.006	0.236	0.001	0.017	0.002	0.009	0.004

	measured	0.29	0.0000	0.0080	0.3563	0.00686	2.70	0.1478	0.00644	0.010	0.2481	0.0012	0.0044	0.00000	0.0116	0.0038
	accuracy	3.794		1041.574	1.797	20.286	-9.076		0.632	64.383	5.108	-2.037	-74.639	-100.000	25.721	-4.266
CGL 006	certified	1.630		0.003	1.839	0.002	7.550		0.004	0.011	0.021	0.174	0.222	0.002	0.010	0.060
	measured	1.37	0.0006	0.0043	1.6583	0.00192	7.46	0.0990	0.00346	0.017	0.0173	0.1637	0.1804	0.00175	0.0092	0.0555
	accuracy	-15.803		63.576	-9.827	-16.620	-1.214		-13.596	48.331	-16.566	-5.908	-18.752	-23.708	-6.020	-7.480
CGL 007	certified	3.870	0.004	0.003	6.888	0.002	3.310	0.101	0.005	0.001	0.006	0.093	1.265	0.002	0.011	0.029
	measured	3.11	0.0031	0.0070	6.5182	0.00194	3.15	0.0884	0.00482	0.000	0.0054	0.0860	1.2067	0.00165	0.0111	0.0281
	accuracy	-19.558	-14.383	119.665	-5.369	-15.526	-4.731	-12.223	-7.216	-70.218	-13.561	-7.215	-4.606	-17.520	-2.646	-2.204
GBM306-12	certified		0.002	1.490	3.595					2.710	0.072				2.063	
	measured	0.82	0.0006	2.9701	4.4817	0.00144	3.23	2.4380	0.00013	2.331	0.0408	0.0035	0.1865	0.01626	2.2145	0.0174
	accuracy		-72.025	99.333	24.664					-13.960	-43.378				7.346	
SARM 1	certified	0.560		0.001	1.400	0.003	4.140	0.016			0.033	0.001	0.054		0.005	0.030
	measured	0.50	0.0005	0.0057	1.4105	0.00278	3.79	0.0112	0.00508	0.005	0.0314	0.0009	0.0485	0.01287	0.0056	0.0276
	accuracy	-10.664		374.474	0.748	3.102	-8.549	-30.265			-3.469	-14.985	-10.194		11.781	-7.984
SARM 41	certified	1.072	0.002	0.005	2.960	0.002	1.154	0.046	0.001	0.003	0.006	0.005	0.330	0.002	0.008	0.015
	measured	0.91	0.0015	0.0150	3.4621	0.00196	1.03	0.0492	0.00078	0.001	0.0060	0.0059	0.3576	0.00135	0.0099	0.0153
	accuracy	-15.109	-1.604	183.861	16.962	-1.934	-10.563	6.945	-2.366	-53.555	1.740	8.678	8.367	-20.697	30.415	4.516

SARM 42	certified	0.636	0.004	0.002	3.270	0.001	0.373	0.077	0.001	0.001	0.002	0.004	0.216	0.001	0.004	0.019
	measured	0.54	0.0018	0.0066	3.4767	0.00100	0.26	0.0833	0.00032	0.000	0.0022	0.0038	0.2487	0.00089	0.0050	0.0205
	accuracy	-14.484	-48.991	288.747	6.321	-16.453	-30.863	8.191	-59.864	-65.119	-0.260	2.608	15.116	-18.801	12.623	6.795
SARM 44	certified	0.100	0.001	0.001	1.440	0.006	0.149	0.023	0.010	0.003	0.001	0.001	1.097	0.008	0.027	0.041
	measured	0.13	0.0005	0.0047	1.5174	0.00624	0.00	0.0185	0.00859	0.002	0.0017	0.0004	1.1499	0.00789	0.0349	0.0450
	accuracy	28.901	-34.471	372.031	5.372	13.387	-99.895	-19.505	-10.476	-41.505	28.346	-16.200	4.824	-6.124	28.860	10.897
SARM 45	certified	0.558	0.004	0.001	8.810	0.004	2.640	0.077	0.003	0.002	0.014	0.009	1.091	0.006	0.007	0.032
	measured	0.47	0.0043	0.0033	8.4130	0.00374	2.65	0.0670	0.00251	0.002	0.0133	0.0085	1.1103	0.00563	0.0084	0.0301
	accuracy	-15.526	5.879	196.354	-4.507	6.791	0.230	-12.996	-7.150	2.759	-6.389	-7.890	1.768	-10.573	13.150	-6.537
SARM 48	certified	6.360		0.001	0.410		3.540	0.015	0.020	0.014	0.029	0.003	0.060	0.044	0.005	0.030
	measured	5.33	0.0001	0.0043	0.4179	0.00247	3.12	0.0090	0.01104	0.020	0.0265	0.0026	0.0215	0.04305	0.0059	0.0285
	accuracy	-16.233		330.690	1.926		-11.975	-40.014	-45.361	45.396	-8.766	-9.651	-64.136	-1.266	10.471	-5.086
SARM 50	certified	7.720	0.004	0.008	7.960		0.510	0.132	0.001	0.003	0.001	0.020	0.516	0.002	0.008	0.009
	measured	6.65	0.0032	0.0148	7.7448	0.00128	0.43	0.1146	0.00062	0.001	0.0011	0.0191	0.5425	0.00211	0.0083	0.0082
	accuracy	-13.885	-20.572	76.316	-2.703		-14.816	-13.213	-38.444	-53.892	-18.851	-1.982	5.137	-8.429	1.894	-4.302
SARM 52	certified	0.264	0.008	0.022	13.780	0.002	0.207	0.209	0.001		0.002	0.003	0.779	0.002	0.026	0.025
	measured	0.29	0.0070	0.0295	13.6642	0.00000	0.16	0.2086	0.00082	0.091	0.0024	0.0024	0.7450	0.00261	0.0291	0.0264

	accuracy	9.137	-13.456	34.751	-0.840	-100.000	-24.716	-0.215	-25.555		21.684	-4.336	-4.364	30.627	10.263	5.547
SARM 69	certified	1.690	0.003	0.005	5.020		1.630	0.100	0.001	0.001	0.007	0.011	0.466	0.003	0.007	0.027
	measured	1.34	0.0028	0.0112	5.2192	0.00160	1.53	0.0976	0.00093	0.001	0.0065	0.0109	0.4840	0.00275	0.0070	0.0293
	accuracy	-20.984	-0.813	143.252	3.967		-5.875	-2.430	3.212	-49.735	-2.022	-0.255	3.872	-5.069	3.201	8.264

Appendix E. Average accuracy for 15 oxides and elements measured within 14 certified reference materials using the UCL pXRF calibration 2 for >10% Ca ceramics. Calculations use the percentage relative error based on a comparison of certified and measured values (Appendix B) but disregard the polarity of the individual accuracy calculations. Averages were based on only those standards whose concentration of the given element falls within the range present in earthenware archaeological ceramics.

Oxide/Element	UCL Cal Ceramics 2 >10% Ca
K_2O	20.92
Sr	9.1
Zr	6.16
TiO_2	17.98
Fe_2O_3	7.07
CaO	14.68
Zn	14.59
Rb	16.99
MnO	16.38
Nb	19.44
Ga	21.57
Co	25.53
Y	23.06
Pb	45.97
Cu	239.37

Appendix F. Descriptions of petrographic fabrics detected in the Wadi Fidan 61 ceramics analyzed in this study.

1. Coarse Granitic Rock-Tempered Fabric
FPN005, FPN006, FPN008, FPN010, FPN011, FPN012, FPN013, FPN015, FPN016, FPN018, FPN019, FPN021, FPN022, FPN023, FPN024, FPN026, FPN027, FPN028, FPN029, FPN030, FPN033, FPN038

This large fabric is characterized by the presence of coarse (up to 4 mm) sub-angular to angular inclusions derived from granitic rock that were added as temper to a non-calcareous clay source of which poorly hydrated remnants remain as inclusions. The dominant igneous inclusions include quartz, weathered plagioclase feldspar, biotite, as well as rock fragments composed of

these three minerals. This material is likely to have derived from coarse grained plutonic rock such as quartz diorite or granodiorite. Perthite is present in some samples (e.g. FPN010, 028) and in some the rock has a medium grain size (e.g. FPN005, 015). The generally angular shape of the granitic inclusions and the bimodality or relative lack of silt-sized grains in most samples could indicate that the coarse material represents crushed weathered igneous rock that was added as temper. However, other rarer inclusion types also occur in the samples, including volcanic rock (e.g. FPN015, 027), chert (e.g. FPN006, 024) and micritic calcite (FPN008, 038). The presence of these inclusions could suggest that angular juvenile eroded sand was added as temper. This material was mixed with non-calcareous clay containing varying amounts of quartz silt. Conspicuous elongate clay-rich inclusions occur in many samples (e.g. FPN011, 026), which appear to be poorly hydrated fragments of the base clay. They can be laminated and have the appearance of mudstone. The samples contain variable amounts of fine silt-sized inclusions deriving from the base clay with some samples being cleaner (e.g. FPN023, 033) and others more silty (e.g. FPN005, 016). Different colored streaks occur in the clay matrix of sample FPN022, though it is not clear whether this is due to intentional mixing or a natural occurrence given the absence of such features in the other samples. The size and proportion of temper varies between samples, with some containing sparser, coarser grains (e.g. FPN033, 038) and others more abundant fine inclusions (e.g. FPN006, 016), comprised primarily of quartz and feldspar. The sherds contain low (e.g. FPN027, 033) to moderate porosity (e.g. FPN011, 022) formed by elongate drying cracks and ring voids around the elongate argillaceous inclusions. Secondary calcite occurs within voids in certain samples (e.g. FPN015, 020). Evidence for the methods used to manufacture the vessels exist in several samples in the form of relic coils, picked out by the orientation of inclusions and voids (e.g. FPN022, 029). The sherds were mainly fired in an oxidizing atmosphere below the vitrification level of the clay minerals (<850°C) and the degradation temperature of calcite (650–750°C). However, some samples exhibit evidence for vitrification (e.g. FPN023, 033) and the breakdown of the calcite inclusions (e.g. FPN018, 038). Some were fired in a poorly oxidizing to reducing atmosphere (e.g. FPN028, 029) and others exhibit core-margin colour differentiation (e.g. FPN021, 038). The elongate clay-rich inclusions present in the Coarse Granitic Rock-Tempered Fabric are also characteristic of the Grog-Tempered Fabric, the Chert-Tempered Fabric and the Argillaceous Fabric, suggesting that they share the same base clay. Inclusions of granitic and volcanic origin occur rarely in other fabrics in this study suggesting further connections in terms of raw materials.

Textural data collected by point counting

	FPN005	FPN011	FPN016
Mineral inclusions	35.5%	26.0%	23.9%
Other inclusions*	-	3.1%	1.8%
Matrix	58.5%	55.1%	64.4%
Voids	6.0%	15.8%	9.8%
Maximum grain size (mm)	1.49	3.99	2.97
Modal grain size (mm)	Coarse sand	Granule	Coarse sand

*Argillaceous

2-- Calcareous Microfossiliferous Limestone Fabric

FPN001, FPN002, FPN003, FPN004, FPN014

The sherds belonging to this homogeneous fabric contain abundant poorly-sorted, sub-angular to rounded inclusions of microfossiliferous limestone (up to 4 mm) and disaggregated bioclasts in a calcareous matrix with rare silt. The dominant limestone inclusions are composed of micrite and foraminifera microfossils. Less common purely micritic inclusions also occur (e.g. FPN004) and are likely to have derived from the same parent rock. It is not clear whether the limestone inclusions were naturally occurring in a chalky clay source eroded from limestone, or added as poorly sorted crushed or eroded rock temper. No areas of incomplete mixing occur to suggest the former. Rare silt-sized quartz, feldspar and chert inclusions occur in the samples which could have been rare components in the limestone, or were present in the base clay, if temper was added. The samples have low porosity, restricted mainly to elongate crack-like voids. Little evidence exists in thin section for the techniques used to form the pottery vessels from which the sherds came. All sherds were fired in an oxidizing atmosphere, though sample FPN004 has a dark core. The maximum sustained temperature was below the dissociation of calcite (c. 650–750°C). Both the Calcareous Microfossiliferous Limestone Fabric and the Plant-Tempered Calcareous Fabric have calcareous clay matrices, though it is not clear whether they share the same raw materials.

Textural data collected by point counting

	FPN014	FPN003
Mineral inclusions	35.5%	38.5%
Other inclusions*	1.5%	2.5%
Matrix	57.0%	57.5%
Voids	6.0%	1.5%
Maximum grain size (mm)	3.51	2.25
Modal grain size (mm)	Fine sand	Coarse sand

*Argillaceous and bioclasts

3. Plant-Tempered Calcareous Fabric

FPN007, FPN009, FPN034, FPN035

This fabric is characterized by the addition of plant temper to calcareous clay with a variable proportion of sand and silt. The plant matter has burnt out during the firing of the ceramics leaving curved voids, some of which contain some charred carbonized remains. In sample

FPN034 the voids have a more circular shape which may be due to different parts of the source plant being added to the pottery from which this sherd derived. It is not possible to identify with certainty the type of plant matter that was added to the pottery of this fabric, however, it could be some sort of grass and perhaps waste from agricultural activity. The base clay to which the organic matter was added was fine and highly calcareous. It contained fine angular quartz (e.g. FPN009) and, in some samples, coarser sand-sized clasts composed of quartz, chert and micrite (e.g. FPN07, 034), rare amphibole (e.g. FPN007) and volcanic rock (e.g. FPN009). The samples are moderately (e.g. FPN009) to highly (e.g. FPN035) porous on account of the voids. Some of the voids are partially infilled with fine gypsum crystals (e.g. FPN035). No clear evidence exists in thin section for methods used to form the parent vessels from which the samples came. Firing was in an oxidising atmosphere and below the dissociation level of calcite (c. 650–750°C). Despite the Calcareous Microfossiliferous Limestone Fabric and the Plant-Tempered Calcareous Fabric having calcareous clay matrices it is not clear whether they share common raw materials, as the inclusions in the latter sherds may be naturally occurring.

Textural data collected by point counting

	FPN009	FPN035
Mineral inclusions	2.0%	3.0%
Other inclusions	-	-
Matrix	84.0%	68.5%
Voids	14.0%	28.5%
Maximum grain size (mm)	0.47	0.60
Modal grain size (mm)	Fine sand	Very fine sand

4. Argillaceous Fabric

FPN020, FPN025, related FPN036

The samples belonging to this fabric are characterized by the presence of elongate clay-rich features as well as lesser quantities of other inclusions in a non-calcareous clay matrix. The clay inclusions, which can be very abundant (e.g. FPN020) appear to be poorly-hydrated fragments of the clay that was used to produce the ceramics. They often have a similar color and seem to have a similar composition to the matrix of the fabric. They can have merging to sharp boundaries as well as ring voids from the shrinkage of the surrounding clay matrix. The elongate shape of the particles as well as the presence of lamination in some is suggestive of mudstone. This appears to have been crushed or collected in a loose eroded state and wetted to create a paste. However, the mix was not sufficiently hydrated leaving many remnant particles. In sample FPN020 some of the clay inclusions have a slightly different color than the matrix and may represent variation within the mudstone source material. Other inclusions occur in the samples, including quartz, angular chert (FPN020), microfossiliferous limestone (FPN036) and rare granitic (FPN025) and

carbonate material (FPN020). Sample FPN025 contains more silt than the other two. It is not clear how the sparse coarser inclusions got into the paste of this fabric. They seem too infrequent to be temper and were not present in the mudstone. The clay matrix is non-calcareous. The samples have low porosity formed mainly by elongate ring voids associated with the argillaceous inclusions. Little evidence exists in thin section for the forming techniques used for these pottery vessels. The ceramics were generally well oxidized during firing and were not subjected to temperatures above the vitrification level of the clay minerals (<850°C), or below the degradation level of calcite (c. 650–750°C). Secondary calcite has been deposited in sample FPN036. The fabric is not homogeneous. Sample FPN036 differs from the other two and contains possible grog inclusions. The mudstone fragments also occur in other ceramics in this study, particularly the Coarse Granitic Rock-Tempered Fabric, suggesting that they share the same base clay as the Argillaceous Fabric. The fabric is also related to the Grog-Tempered Fabric on account of the presence of possible grog in two samples (FPN025 and 036).

Textural data collected by point counting

	FPN025
Mineral inclusions	9.1%
Other inclusions*	13.5%
Matrix	67.4%
Voids	10.0%
Maximum grain size (mm)	1.13
Modal grain size (mm)	Medium sand

*Argillaceous

5. Grog-Tempered Fabric

FPN017, FPN031, FPN037

This fabric is characterized by the addition of coarse inclusions of crushed pottery or ‘grog’ (up to 1 mm) in a non-calcareous matrix. The grog inclusions have a generally angular shape and can be surrounded by ring voids. They vary in terms of their fabric both between and within sherds, for example sample FPN017 contains grog with both a fine clean fabric and a silty fabric. Sample FPN031 contains grog with calcareous inclusions. Other inclusions include elongate laminated argillaceous fragments of poorly hydrated base clay (samples FPN017, 037), primary calcite (samples FPN017, 037), woody material (sample 031) and fine quartz and feldspar. It is not clear how these other coarser inclusions got into the paste of this fabric. The fabric has a non-calcareous clay matrix. The samples can have high porosity due to the presence of ring voids around the frequent grog (e.g. sample FPN017). Evidence for coiling is visible in sample FPN031 in thin section. Firing was variable, ranging from below the vitrification level of the

clay minerals (<850°C) and degradation level of calcite (c. 650–750°C) in sample FPN031 to above these in sample FPN017. Sample FPN017 was well oxidized whereas the other two were not. Secondary calcite has been deposited in all three samples, particularly FPN031. The presence of elongate argillaceous fragments in the Grog-Tempered Fabric links it to other samples in this study belonging to the Argillaceous Fabric and the Coarse Granitic Rock-Tempered Fabric. They may share the same base clay, which was prepared by crushing and hydrating mudstone, the remnants of which remain in the pottery. The presence of possible grog in some Argillaceous Fabric samples further links the Grog-Tempered Fabric with these sherds.

6. Chert-Tempered Fabric

FPN032

This single sample is characterized by a fabric containing abundant, poorly sorted sub-angular to sub-rounded angular chert inclusions (up to 3mm) in a non-calcareous clay matrix. The chert can be iron-stained or clear and may contain chalcedony. It appears to have been added as temper. Silt-sized quartz inclusions, rare micritic calcite and elongate argillaceous inclusions are also present in the sample. The sample has a non-calcareous clay matrix that contains some streaking. This could be due to intentional mixing, but is more likely to be a natural occurrence. The sample has low porosity formed by occasional elongate drying voids. Possible coils exist in thin section that are suggestive of the technique used to form the parent vessel from which the sherd originated. Firing appears to have been above the degradation temperature of calcite (*c.* 650–750°C) and was incompletely oxidizing, leaving a dark core. The sample contains post-depositional secondary phenomena. The presence of elongate argillaceous fragments in the Chert-Tempered Fabric links it to other samples in this study, such as the Argillaceous Fabric and the Coarse Granitic Rock-Tempered Fabric. Chert is present in other sherds, such as sample FPN020 from the Argillaceous Fabric.